The mechanical properties of type II superconducting materials are reviewed as well as the effect of stress on the superconducting properties of these materials. The bcc alloys Nb-Ti and Nb-Zr exhibit good strength and extensive ductility at room temperature. Mechanical tests on these alloys at 4.2 K revealed serrated stress-strain curves, non-linear elastic effects, and reduced ductility. The non-linear behaviour is probably due to twinning and de-twinning or a reversible stress-induced martensitic transformation. The brittle A-15 compound superconductors, such as Nb_3Sn and V_3Ga, exhibit unusual elastic properties and structural instabilities at cryogenic temperatures.

Multifilamentary composites consisting of superconducting filaments in a normal metal matrix are normally used for superconducting devices. The mechanical properties of alloy and compound composites, tapes, as well as composites of niobium carbonitride chemically vapour deposited on high strength carbon fibres are presented. Hysteretic stress-strain behaviour in the metal matrix composites produces significant heat generation, an effect which may lead to degradation in performance of high field magnets. Measurements of the critical current density, J_c, under stress in a magnetic field are reported. Modest stress-reversible degradation in J_c is observed in Nb-Ti composites while more serious degradation is found in Nb_3Sn sample.

The importance of mechanical behaviour on device performance is discussed.

A review of mechanical behaviour and stress effects in hard superconductors

C.C. Koch and D.S. Easton

The mechanical behaviour of superconducting materials has been of interest and concern to researchers in this field over the last two decades since the discovery and use of 'hard' high field superconductors. The inherent brittleness of many of the high field superconductors, for example, compounds with structures of type A-15, B-1, or C-15, etc, required the development of unique processing techniques for manufacture of practical conductors. Fundamental studies of the effects of mechanical stress on superconducting properties provide insight into the nature of superconductors. In recent years, an increased interest in the mechanical behaviour of commercial superconductors has occurred because of the large mechanical forces expected in proposed superconducting devices such as magnets for plasma confinement and energy storage, rotating machinery, and electrical transmission lines. At several laboratories facilities have been developed to study the effects of mechanical stress *in situ* on superconducting properties. Results from such measurements have become available within the last year, thus, it is appropriate to review the existing knowledge of mechanical behaviour and stress effects in 'hard' superconductors. The term 'hard' used in this review is an imprecise but useful term often applied to type II superconductors which have high values of the upper critical field, H_{c2} and high values of J_c, the critical current density. These superconductors are the ones at present used or potentially useful for electrical engineering applications. This review will cover the mechanical properties of superconducting alloys and compounds at ambient and low temperatures, the effects of stress on superconducting properties, and their implications for superconducting applications.

The authors are with the Oak Ridge National Laboratory, Metals and Ceramics Division, Oak Ridge, Tennessee 37830, USA. Received 1 March 1977.

Mechanical behaviour of alloy superconductors

For the purposes of this review the hard superconducting alloys are bcc Nb-Ti and Nb-Zr. At present the commercial superconductor most freely available is Nb-Ti which superseded Nb-Zr alloys about ten years ago, partly due to its better mechanical properties as well as its higher values of H_{c2}.

Elastic behaviour of hard superconducting bcc alloys

Elastic constants on single crystals of the commercial superconducting alloy Ti-40 at % Nb were determined at 298 K by Reid et al.[1] The results of these measurements were c_{11} = 56.5 GPa, c_{12} = 111.6 GPa, $c' = (c_{11} - c_{12})/2$ = 22.47 GPa, and c_{44} = 39.63 GPa. From these values the following moduli were calculated: bulk modulus, K = 126.6 GPa, shear modulus on $<111>$ slip systems, G = 26.26 GPa, and Zener's anisotropy factor $A = c_{44}/c'$ = 1.763. Thus the elastic properties are only slightly anisotropic and isotropic elasticity theory should apply to calculations such as those for dislocation strain fields. Attempts to measure the elastic constants at lower temperature were unsuccessful due to an unexplained due to an unexplained high attenuation of the shear wave below ~ 270 K. No change in the bcc crystal structure was observed by x-ray diffraction techniques at temperatures as low as 78 K. The polycrystalline Young's modulus can be estimated from this single crystal data using the averaging techniques of Voigt[2] or Reuss.[3] Experimental results on polycrystalline

samples in uniaxial tension lie between these two extreme analyses with the measurements on wire sample with cellular fibres parallel to the tensile axis more closely approcimating the Voigt average.[2] The values are $E_{Voigt} = 9.047 \times 10^{10}$ N m^{-2} and $E_{Reuss} = 8.431 \times 10^{10}$ N m^{-2}.

Elastic moduli of polycrystalline Nb-Ti alloys have been measured by acoustic techniques and from stress–strain curves (Table 1). Room temperature values vary with niobium concentration (Fig. 1). The values depend on the microstructure, that is, the sample heat treatment. A broad minimum in E is observed at the Ti-rich part of the alloy system. The values measured for E at 4.2 K are ~ 12–15% higher than the room temperature values.[4,5]

Nelson et al[13] measured Young's modulus for a series of Zr-rich alloys (0–25 at % Nb) on polycrystalline and single crystal samples using the composite resonator acoustic technique. The room temperature values of E for Zr–25 at % Nb (~ 6.8×10^{10} N m^{-2}) are similar to the values for a Ti–25 at % Nb alloy (see Fig. 1) and the increase in E with decreasing temperatures is comparable. Both alloy systems exhibit a minimum in E with composition in the range of 20–30 at % Nb. In the work of Nelson et al the alloys with 12–25 at % Nb were two phase, bcc + omega. It was concluded that the omega phase had a slightly higher modulus than the bcc phase since thermomechanical treatments which increased the amount of omega phase also increased E.

However, Sekula and Redman[14] found E to decrease by ~ 9% from room temperature to 77 K in measurements made from uniaxial stress–strain curves.

The shape memory effect and pseudoelasticity in hard superconducting bcc alloys

Two related phenomena – the shape memroy effect (SME) and the pseudo-elastic effect – are observed in a wide range of alloy systems in which reversible martensitic transformations occur (for example, reference 15). The SME is described by the observation that a specimen containing deformation induced martensite will change its shape to the

Table 1. Young's modulus for Nb-Ti alloys

Nb-Ti Alloy (at % Nb)	E (N m^{-2} x 10^{10})	Reference number	Remarks
40.0	6.9	4	
38.5	5.5	5	
42.5	9.3	6	
49.0	9.7	6	
61.0	10.2	6	
74.0	10.6	6	
82.5	10.9	6	
91.0	10.9	6	
36.0	7.4	7	
38.5	7.8	7	
23.0	6.3	8	95% cold-work
34.0	7.2	8	95% cold-work
34.0	7.8	8	annealed 1000°C
44.0	8.1	8	95% cold-work
44.0	8.8	8	annealed
36.0	8.2	9	
38.5	8.3	9	
36.0	8.6	10	
34.0	9.1	11	measured at 4.2 K
34.0	8.1	11	normalized to room temperature
6.5	7.8	12	as-quenched
8.0	6.2	12	as-quenched
8.0	9.8	12	annealed
11.5	7.8	12	as-quenched
18.0	9.5	12	as-quenched
21.0	7.8	12	as-quenched
25.5	6.6	12	as-quenched
25.5	8.1	12	annealed
29.0	7.8	12	annealed
38.0	7.9	12	as-quenched
43.5	8.4	12	as-quenched
43.5	9.0	12	annealed

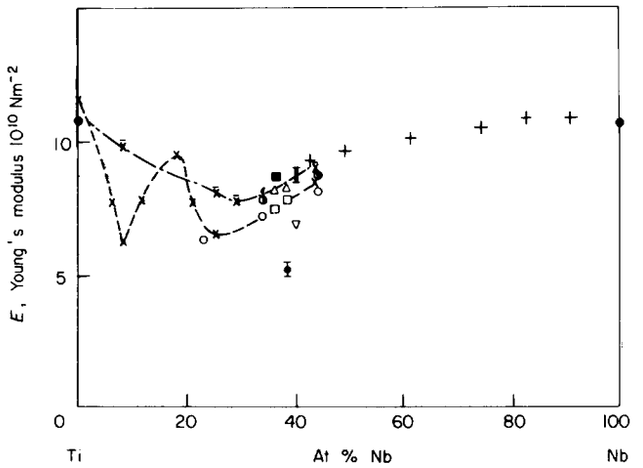

Fig. 1 Young's modulus of Nb-Ti alloys (room temperature)
Bulk samples: X̄–X̄ – annealed; X–X – as quenched (both from Fedotor); + – Nedyukha & Chernyy (arc melted); ▮– Reid et al; □ – Ledbetter; ○ – Albert & Pfeiffer (95% cw); ◑ – Albert & Pfeiffer (recrystallized at 1000°C); △ – Easton & Koch
Wire samples: ⧗ – Reed et al; ▼ Rutherford Laboratory; ■ – Easton; ◖ – Schmidt (4.2 K, normalized to 298 K)

original (predeformation) dimensions when the reverse martensitic transformation is activated by heating above some reversion temperature. In the pseudoelastic effect, a shape change (strain) occurs by development and growth of martensitic plates during continuous application of stress, which revert and disappear when the load is removed. The effect often produces a non-linear stress–strain curve with a hysteresis loop on stress reversal.

These effects differ from system to system and can be produced by the stress-induced reorientation of the twin domains within martensitic plates in addition to the stress-induced formation of the plates themselves. Such effects have been observed during deformation both above and below M_s (the temperature below which martensite forms).

One example of each effect has been reported for Nb-Ti alloys. Baker[16] described evidence for the shape-memory effect in a Ti-22 at % Nb (35 wt % Nb) alloy. (This is a composition which has been used as a commercial superconductor.) In this alloy, an orthorhombic martensite, α'', phase is formed at $M_s \approx 175°C$ when the material is quenched from the single-phase β (bcc) field (temperatures $> \sim 700°C$). If the fully martensitic alloy is deformed below M_s it recovers its original shape when heated above the reversion temperature, $A_s \approx 184°C$. In the fully martensitic condition the strain is accomplished by the preferential growth of those α'' variants which result in stress relief (the orientation relationship between the β and α'' predicts twelve equivalent α'' orientations from a single β orientation).

Easton and Koch[17] presented evidence for the pseudoelastic effect in Ti-36 at % Nb and Ti-38.5 at % Nb alloys (commercial compositions) at low temperatures. Uniaxial tensile stress–strain curves at 4.2 K exhibited non-linearity with recovery of strain on unloading (Fig. 2). At higher strains load drops were observed and serrated stress–strain curves were obtained. More discussion of these serrations will be presented in the next section. Acoustic noise was also observed in these experiments. Almost immediately upon application of stress at 4.2 K audible 'clicks' could be detected. The frequency of clicks was greatest at low stresses, both during loading and unloading. If a sample were loaded to a given stress and then unloaded, no clicks were heard until the stress had dropped below a certain value. When the test temperature was raised, the audible clicks and the serrations in the stress–strain curve disappeared at temperatures above ~ 30 K. This behaviour is the same phenomenologically as that observed in alloys which exhibit pseudoelasticity.[18] Such evidence and the observations of ductility[9] point to the presence of either a stress-induced martensitic transformation or reversible twinning. It is possible that this martensite is the α'' phase. Consider the M_s versus composition curve for Nb-Ti alloys, presented in Fig. 3 from the data of Duwez,[19] Brown et al,[20] and Baker.[16] A reasonable extrapolation of the M_s curve to 36–39 at % Nb indicates the M_s temperature could occur near 4.2 K. Since the M_d temperatures (the temperature below which deformation induced

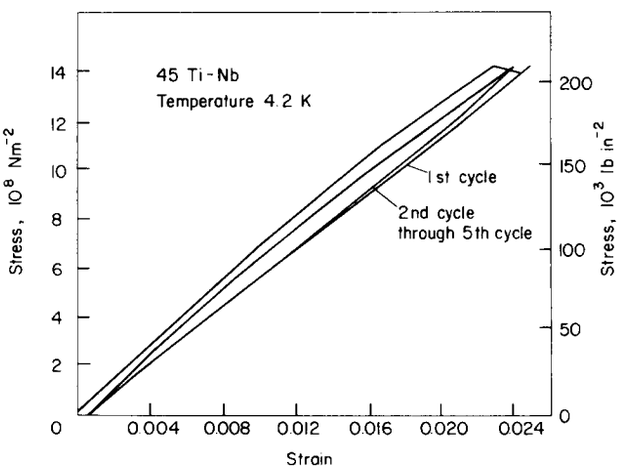

Fig. 2 Stress–strain curve of a Ti-38.5 at % Nb alloy at 4.2 K

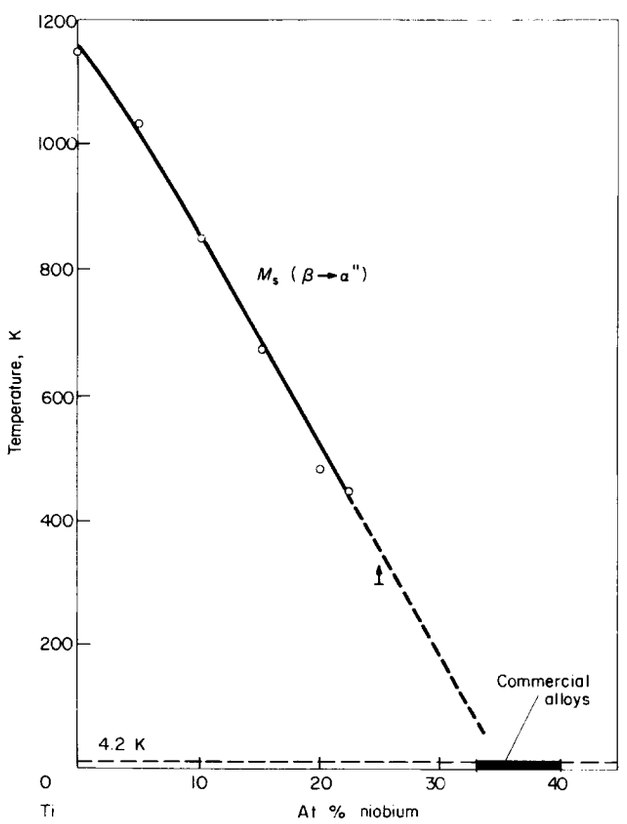

Fig. 3 M_s curve for α'' in Nb-Ti alloys

martensite forms) usually lies above M_s, it is plausible that stress-induced α'' could occur in these alloys. It is also possible that the martensite is stress-induced hcp α (the equilibrium phase) or some other intermediate phase. Since any such stress-induced phase would revert to the usual phase below room temperature, metallurgical studies of these alloys under stress at low temperatures are required and several groups,[21,22] have initiated such studies.

The non-linear stress–strain curve and hysteresis loops are also observed in Nb-Ti/Cu (and other matrices, such as CuNi and Al, etc) multifilamentary composites even at room temperature. This is due to the composite behaviour itself which will be discussed in the section on mechanical behaviour of composites. However, it should be emphasized that at helium temperatures the Nb-Ti *itself* is capable of exhibiting this pseudoelastic behaviour.

The authors found similar effects (serrated stress–strain curves and hysteretic, non-linear recovery of strain on unloading) in both a composite consisting of Nb–25% Zn filaments in a copper matrix and a bare filament of the Nb-Zn with the copper removed. Although no evidence of the shape-memory effect in Nb-Zn could be found in the literature, no comprehensive study has been made in this area.

Table 2. Plastic properties of bcc superconducting alloys

Alloy	Test temperature, K	Condition	Yield strength, $N\,m^{-2} \times 10^8$	Tensile strength, $N\,m^{-2} \times 10^8$	Reduction in area, %	Elongation, %	Reference
Nb-25 at % Zr 0.25 mm dia wire	289	cold-worked	16.1		51		Fox & Pryle[38]
	77	cold-worked	19.8	24.4	35		Fox & Pryle
	4.2			30.3	21		Fox & Pryle
0.13 mm dia wire	298	cold-worked	17.7	19.1	16		Fox & Pryle
	77		24.3	25.2	16		Fox & Pryle
	4.2			40.4	14		Fox & Pryle
Ti-40 at % Nb 0.17 mm dia wire	300	cold-worked	8.8	9.8		0.3	Verkin et al[34]
	77	cold-worked	15.2	15.7		0.55	Verkin et al
	21.3			22.8		0.3	Verkin et al
	4.2			16.7		0.1	Verkin et al
Ti-50 at % Nb 0.15 mm dia wire	300		16.2	16.2		0.2	Verkin et al
	77		18.6	19.8		0.45	Verkin et al
	4.2		18.6	19.1		0.30	Verkin et al
Ti-38.5 at % Nb	298			7.8		2.2	Reed et al[36]
	77			10.2		2.2	Reed et al
	4.2			12.8		2.2	Reed et al
Ti-36 at % Nb 0.213 mm dia wire	300	cold-worked		11.1	22	2.3	Easton & Koch[17]
	4.2	cold-worked		21.6	7	4.5	Easton & Koch
Ti-36 at % Nb 0.267 mm dia wire	300	cold-worked		10.3	20	1.2	Easton & Koch
	77	cold-worked		17.3	17	2.4	Easton & Koch
	4.2			22.1	8	4.8	Easton & Koch
Ti-36 at % Nb 0.318 mm dia wire	300	cold-worked		13.8	15	4.1	Easton & Koch
	4.2	cold-worked		21.6	12	4.8	Easton & Koch
Ti-36 at % Nb 1.98 mm	300	800°C anneal		5.0	71	8.8	Easton & Koch

Alloy	Test temperature, K	Condition	Yield strength, $N\,m^{-2} \times 10^8$	Tensile strength, $N\,m^{-2} \times 10^8$	Reduction in area, %	Elongation, %	Reference
	4.2			15.1	11	<0.2	Easton & Koch
Ti-38.5 at % Nb 1.98 mm dia tensile sample	300	800°C anneal		5.0	77	9.6	Easton & Koch
	77			11.0	47	3.3	Easton & Koch
	4.2			15.1	7	<0.2	Easton & Koch
Ti-34 at % Nb 0.25 mm dia	300	cold-worked	8.6–8.7	8.8		3.0–3.5	Hillmann[30]
Tensile sample	300	cold-worked 50%	4.0†	7.2		9.0	Hillmann
Tensile sample	4.2	cold-worked 50%	12.3	14.5		0.5	Hillmann
Ti-25 to 50 at % Nb 0.25 mm dia wire	300	cold-worked		6–7			Bychkova et al[39]
Ti-25 at % Nb		10 h at 450°C		14.6			Bychkova
Ti-25 at % Nb	300	cold-worked		6.6			Bychkova et al[40]
Ti-65 at % Nb Wire	300	cold-worked		7.9			Alekseevskii et al[41]
	77			13.7			Alekseevskii et al
	20			18.8			Alekseevski et al
Nb-33 at % Zr 0.17 mm dia wire	300	cold-worked		19.2			Easton[10]
	4.2			29.0			Easton

* Not defined-non uniform deformation

† Elastic limit.

Plastic behaviour of hard superconducting bcc alloys

This section discusses the 'plastic' properties of Nb-Ti, Nb-Zr, and related alloys. These properties include those defined by conventional engineering stress–strain curves, such as the elastic limit, yield strength, ultimate tensile strength, and percent elongation at fracture. Plastic properties data are available for a range of Nb-Ti alloys at ambient and lower temperatures. Data on bcc superconducting alloys is presented in Table 2. Body-centred-cubic metals and alloys typically exhibit a marked temperature dependence on their mechanical properties.[23] This temperature dependence includes a large (2–3 times or more) increase in yield and ultimate tensile strength as the temperature is decreased and also includes a loss of ductility at low temperatures. This general behaviour is observed in the Nb-Ti and Nb-Zr alloys. The largest quantity of data, and those most easily reproduced, are for the ultimate tensile strength. Even though this parameter is sensitive to composition and metallurgical history, selected values have been plotted versus test temperature in Fig. 4 for Nb-Ti and Nb-Zr alloys. It is clear that, in general, Nb-Zr alloys exhibit higher ultimate tensile strengths than Nb-Ti alloys. Yield strengths at low temperatures are difficult to measure and/or define due to the limited ductility and the nature of the stress–strain curve.

Serrated stress–strain curves. Most investigators report serrated stress–strain curves at low temperatures in these alloys. An example of a serrated stress–strain curve is presented in Fig. 5 for Ti-36 at % Nb.[16] Various explanations have been given for serrated stress–strain curves which occur at low temperatures. These include twinning,[24] stress-induced phase transformations,[25] 'burst' dislocation formation,[26] and 'adiabatic deformation'. Basinski[27,28] has shown that adiabatic deformation is a common feature of many metals at liquid helium temperatures. Since the specific heat of metals becomes quite small at low temperatures, an energy input, such as strain energy, can produce a local rise in temperature. If the flow stress decreases rapidly with temperature, the decrease in flow stress caused by local heating may exceed the increase due to work-hardening. This instability produces a load drop, the sample cools, and the process repeates itself and gives rise to the serration.

Evans[29] attributed the serrated stress–strain curves in Ti-40 at % Nb at 4.2 K to adiabatic deformation. Hillman[30] attributed the serrations he observes at 4.2 K in Ti-34 at % Nb alloys to a localization of slip on the principal slip planes, {110}, due to the restricted ability for cross-slip at low temperatures. He suggests such slip processes would give rise to the serrations but does not rule out the possibility of twinning

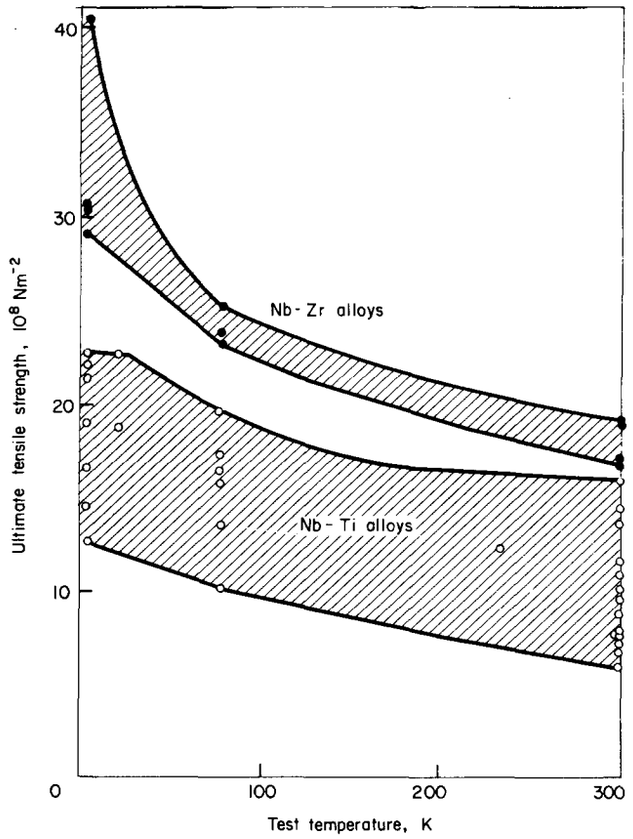

Fig. 4 Selected ultimate tensile strength values of Nb-Ti and Nb-Zr alloys versus temperature

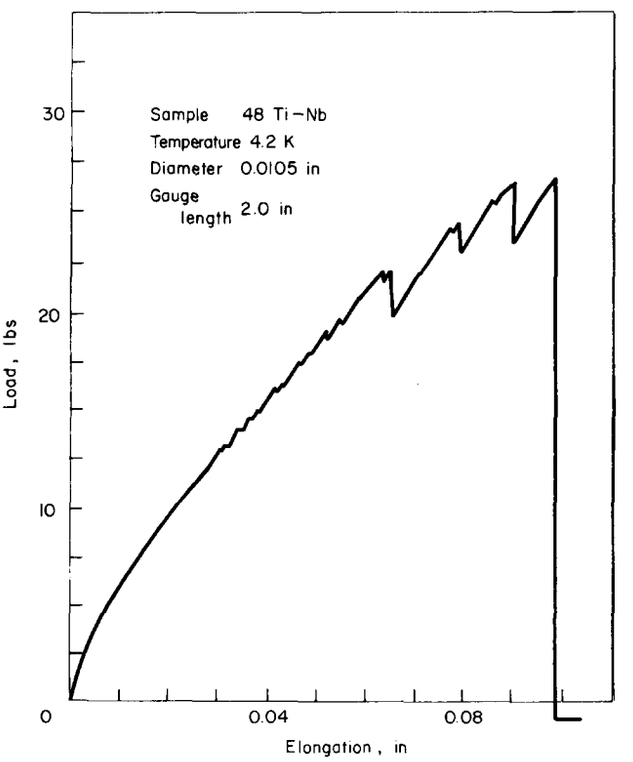

Fig. 5 Load-elongation curve of a Ti-36 at % Nb alloy at 4.2 K

and/or adiabatic deformation. However, Albert and Pfeiffer[33] propose that it is slip exclusively on {100} planes which is responsible for the load drops. They do not elaborate on the mechanism(s) responsible. The common slip plane for bcc metals is {110}, but Albert and Pfeiffer assume the {100} slip planes are active because of the <100> fibre texture of the samples and the fact that shear fracture occurs at a 45° angle to the tensile axis. However, this geometrical argument is not unique, and the possibility of twinning as a deformation mode is not considered so this assumption is of doubtful validity.

Yajima and Ishii find serrated stress–strain curves, which they attribute to twin deformation,[32] in Nb-26 and 42 at % Zr at temperatures below 201 K. Twinning is a common mode of deformation in bcc metals and alloys at low temperatures. Flewitt and Palmer[33] find the upper temperature limit of twin formation varies with Zr concentration in Nb-Zr alloys, reaching a maximum slightly above room temperature for a Nb-25 at % Zr alloy. Single surface trace analyses were consistent with a {112} habit plane for the twins at all temperatures and compositions. They observed microstructural evidence for detwinning after raising the temperature. At 4.2 K twinning became the deformation mode for plastic yielding.

Serrated stress–strain curves are also observed in the measurements of Verkin et al[34] on Ti-40 at % Nb and Ti-50 % Nb wires at 4.2 K. They saw a decrease in the ultimate tensile strength as the temperature decreased from 22 K to 4.2 K. This effect was also reported by Albert and Pfeiffer[31] for the Ti-34 at % Nb alloy after 40% cold-work, but not in a sample deformed only 50%. Reed and Mikesell[35] have seen this effect in several Cu-base fcc alloys. They proposed that the stress needed to nucleate twins decreases with decreasing temperature and that deformation at 4.2 K occurs mainly by twinning.

The only study found which did not report serrated stress–strain curves in Nb-Ti alloys at 4.2 K was that of Reed et al.[5] However, subsequent measurements revealed serrations[36] and the reasons for this disagreement are not known. Serrations are usually only detected if a 'hard' testing machine is used[37] so that experimental conditions must be considered in any conclusions regarding the occurence or not of serrations at low temperatures.

Serrated stress–strain curves were reported by Schmidt[11] for Ti-34 at % Nb wires (0.26 mm diameter) at 4.2 K. In some cases he observed serrations during unloading as well as during loading. Easton and Koch[17] reported serrations at 4.2 K in Ti-36 at % Nb and Ti-38.5 at % Nb samples in the form of 2 mm diameter tensile samples and in several sizes of wire etched from multifilamentary conductors. They also observed serrations with both increasing and decreasing load. Acoustic noise, as audible 'clicks', accompanied the occurence of the serrations. The clicks preceded the first serrations on loading. On unloading neither clicks nor serrations were noted until the stress had dropped to a given level then both occurred.

While any of the mechanisms listed above for serrated stress–strain curves at low temperatures could explain the serrations on loading, only a reversible, stress-induced (martensitic) phase transformation or stress-reversible twinning can explain the serrations on unloading. It is thus

concluded that the serrations in Nb-Ti alloys are due to one of these two phenomena. *In-situ* x-ray diffraction or electron microscopy will be required to decide which mechanism is operative.

Ductility. In general, there is a loss of ductility in Nb-Ti and Nb-Zr alloys at liquid helium temperatures. The degree of this effect depends on specimen size, condition, and ductility parameters (see Table 2). Percent reduction in area, measured after fracture, exhibited a marked decrease. In tensile specimens, percent elongation also decreased.[9] However, in wire samples elongation values at 4.2 K were either comparable to those at 298 K or greater (Table 2). One reason for this apparent anomaly is as follows. Most of the deformation at 4.2 K occurs with the discontinuous load drops. If this is twinning or martensite formation, the twin (martensite) plate can propagate across the sample diameter and produce deformation. Such deformation might be restricted in larger samples and the twin (martensite) plate intersections can initiate cracking.

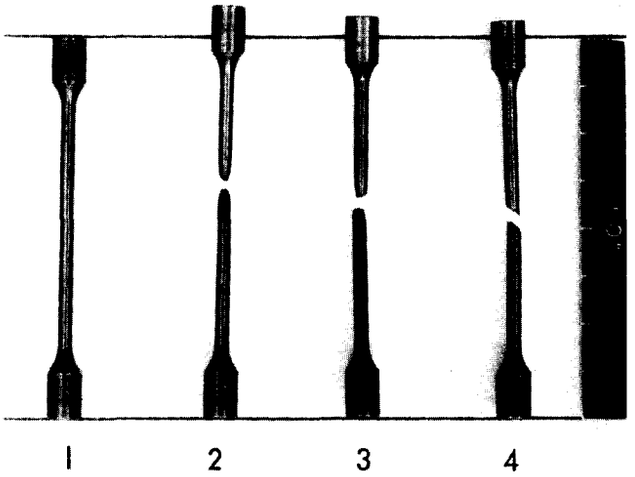

Fig. 6 Tensile specimens of Ti-38.5 at % Nb alloy fractured at various test temperatures
1—Before testing; 2—300 K; 3—77 K; 4—4.2 K

Fig. 7 Fracture surface of a 2 mm diam Ti-38 at % Nb specimen tested at 4.2 K

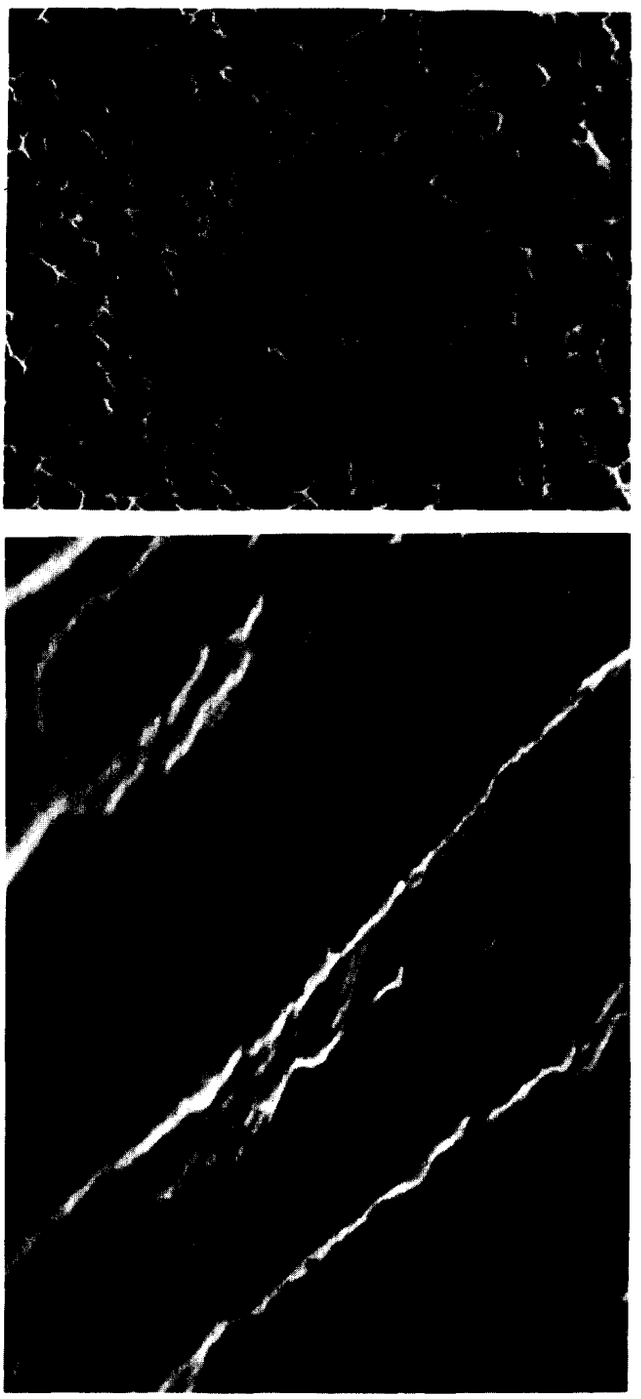

Fig. 8 a—Typical 4.2 K fracture surface of a Ti-38.5 at % Nb specimen SEM micrograph 3000x; b—A small portion of the sample in Fig. 8a showing some evidence of brittle fracture. SEM 10 000x

The appearance of the fracture surface changes with test temperature (Fig. 6). At room temperature the familiar ductile 'cupe and cone' fracture is observed. This mode of fracture persists at 77 K although less necking is observed. At 4.2 K a shear fracture at $\sim 45^\circ$ to the tensile axis occurs (Figs 6 and 7). However, the microscopic features of this fracture indicate the mechanism can be classified as ductile fracture of the shear rupture type. Scanning electron micrographs (Fig. 8a) of the fracture surface reveal a finely dimpled surface characteristic of microscopic ductile failures. Small areas in the fracture surface do show evidence of brittle failure (Fig. 8b). Evidence for inter- and transcrystalline brittle fracture was presented by Flewitt and Palmer[33] for Nb-Zr alloys at lower test temperatures. Scanning electron micrographs of fractured surfaces on samples with low ductility (low temperatures) exhibit some cleavage facets of {100} type. Some cracks are apparently nucleated by {112} twins. Such cracks first propagate on {110} planes before reverting to the {100} cleavage plane. A ductile-brittle transition temperature was determined by studying the nature of the fracture surfaces and found to be a maximum for the Nb-25 at % Zr composition. Takaai[42] observed the ductile to brittle transition temperature in Nb-30 at % Zr to be $\sim 250^\circ$C. Additions of Ti($\sim$ 10 at %) decreased the transition temperature to $\sim -50^\circ$C. Further Zr additions had similar effects. There was no obvious correlation between oxygen content and ductility for concentrations up to $\sim$ 800 ppm. However, Courtney and Wulff[43] found oxygen contents of $\sim$ 3000 ppm severely embrittled Ti-45 at % Nb samples.

Microstructures. There have been several electron microscopy studies of the room temperature deformation structures of Nb-Ti and Nb-Zr alloys. Neal et al[44] observed a well defined dislocation cell structure in Ti-40 at % Nb cold-worked at room temperature. Pfeiffer and Hillman[45] observed elongated dislocation cell structures which they define as 'substrips' or 'microstrips' in Ti-22 at % Nb and Ti-34 at % Nb alloys. The fibre texture was $<110>$ and the substrip width was 90 to 500 Å. Reuter et al[46] also observed the $<110>$ fibre axis texture in a Ti-45.7 at % Nb alloy wire deformed 99.9% by cold work. This severe deformation could be attained in spite of the presence of 2390 ppm of oxygen in the sample. A diffuse tangle cell structure was seen, having a 0.2 μm average cell diameter. Witcomb and Dew-Hughes[47] observed a heterogeneous microstructure in cold-worked ($>$ 90%) Ti-35 at % Nb strip containing 400 ppm nitrogen and 3000 ppm oxygen. Some regions examined contained a uniform high dislocation density while other regions exhibited the cellular structure with a cell diameter ~ 0.3 μm. Baker[48] noted a significant difference between the microstructures of Ti-40 at % Nb sheet samples with and without nitrogen doping (480 ppm Ng). The undoped samples exhibited a diffuse cellular structure with a $\geqslant 0.25$ μm cell diameter. The nitrogen-doped samples had a much more uniform dislocation density and no evidence for the cell structure was observed.

Walker et al[49] presented microstructural results on cold-rolled Nb-25 at % Zr sheet. They found tangles and stringers of dislocations in the as-worked condition. Heating between 500–900°C produced a well-defined cell structure. The typical bcc rolling texture was obtained with (100) planes parallel to the rolling plane and [100] directions parallel to the the rolling direction. Milne[50] studied 0.25 mm diameter wires removed from multifilamentary Nb-25 at % Zr conductors. A fibrous, diffuse dislocation structure was observed which sharpened into a well-defined cell structure during annealing. Narlikar and Dew-Hughes reported[51] a cellular structure in cold-worked ($>$ 90%) Nb-25 at % Zr, with a cell size ~ 0.5 μm. They noted a similar cell structure, with a slightly smaller average cell diameter (~ 0.4 μm) in cold-worked Nb-25 at % Ti. However, Finlayson and Milne[52] saw no evidence for the cellular structure at room temperature in either Nb-26 at % Zr or Nb-32 at % Zr cold-rolled up to 96%. From these observations, it was concluded that cross-slip is difficult in these alloys.

Flewitt and Palmer[33] have carried out a detailed microstructural analysis of Nb-Zr alloys with Zr content 16 to 40 at %. Their TEM results reveal slip on {110} planes with some additional slip on {112} during room temperature deformation. Some evidence for wavy coarse slip lines is also presented. As the deformation temperature was raised above ambient, more wavy slip lines were observed along with the higher ductility. At temperatures above $\sim$ 100–200°C depending on Zr concentration) a cellular dislocation distribution was observed (see Fig. 9). At temperatures below room temperature slip was chiefly on {110} planes with dislocations confined to bands with a uniform distribution within the bands. Additions of Zr gave the same effect on dislocation structure as lowering the temperature in the composition range 0 to 25 at % Zr. The reverse was observed for alloys from 25–40 at % Zr (see Fig. 9). Twinning became an important mode of deformation at lower temperatures. The effect of temperature and composition on twinning is illustrated in Fig. 10. As 4.2 K is approached twinning became the major deformation mode for yielding

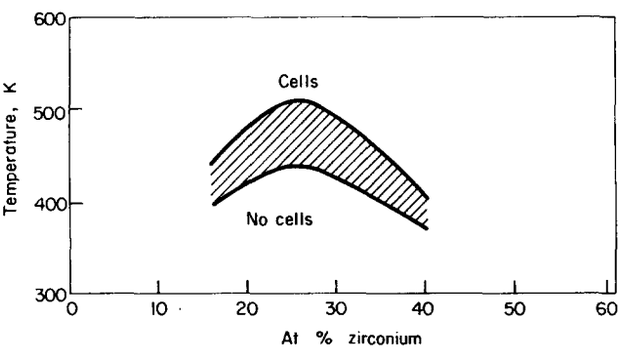

Fig. 9 The effect of temperature and composition on dislocation structure in Nb-Zr alloys (after Flewitt and Palmer[25])

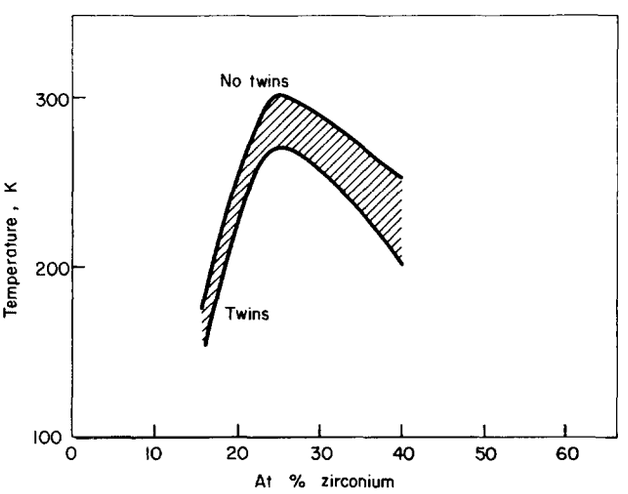

Fig. 10 The effect of temperature and composition on twinning in Nb-Zr alloys (after Flewitt and Palmer[33])

and at 4.2 K yield and fracture were coincident. Some crack nucleation was observed at twin intersections and thus twinning influences the fracture process as discussed above.

From the above survey of plastic properties of bcc hard superconductors, it is apparent that strength and ductility are sensitive to test temperature, composition, interstitial impurity level, sample size, and metallurgical structure.

At room temperature, Nb-Zr alloys are stronger and perhaps somewhat less ductile than Nb-Ti alloys. At liquid helium temperatures both systems exhibit limited ductility and show serrated stress–strain curves, twinning, and perhaps stress-induced martensitic transformation.

Mechanical behaviour of composite bcc superconductors

Thermal mechanical and/or electromagnetic instabilities make it impossible to use the full current-carrying capability of hard superconductors in applications such as high field magnets.[53] Practical superconductors therefore require stabilization by incorporation of one or more normal conductors with the superconductor. In the case of the bcc superconducting alloys, the composite usually takes the form of multiple filaments of superconducting wire encased in a normal metal matrix. The matrix material is typically a high-conductivity metal such as copper or aluminium. For a more complete decoupling of the filaments they are usually twisted or transposed for pulsed field applications. A more resistive Cu-Ni alloy matrix is also used under pulse-field conditions. State-of-the-art conductors now are complex composites consisting of up to 10 000 or more 10 to 20 μm diameter filaments, often in a mixed Cu/Cu-Ni alloy matrix. The mechanical properties of the composite are the relevant quantities to be considered for superconducting applications.

Many review articles[54-56] have appeared during the last ten to fifteen years on the mechanical behaviour of composite materials. No attempt will be made here to review this broad subject but a few comments relevant to superconducting composites will be made before the experimental situation is presented. In general it has been possible to predict mechanical properties of composites from the corresponding properties of the component materials.[54] The basis of this approach is continuum mechanics and the result is the well-known 'rule of mixtures' relationship for a property in terms of the volume fractions of each phase in the composite. The assumptions which are usually made in order to apply this analysis are[55]

1. isostrain conditions exist in each phase at all stresses;
2. the fibres are aligned parallel to the loading axis;
3. a 'perfect' bond exists between the fibre and matrix;
4. the properties of the phases are unaltered in the combined state;
5. no transverse stresses develop as a result of fibre matrix interaction, and
6. no residual stresses exist in either component prior to loading.

While the rule of mixtures has been verified experimentally in many systems,[54] the above assumptions do not always hold true in practice. When this occurs, significant deviations from the rule of mixtures are observed.[54] The tensile stress–strain of a composite (strong fibres, weak matrix) goes through through four stages,[56] (see Fig. 11):

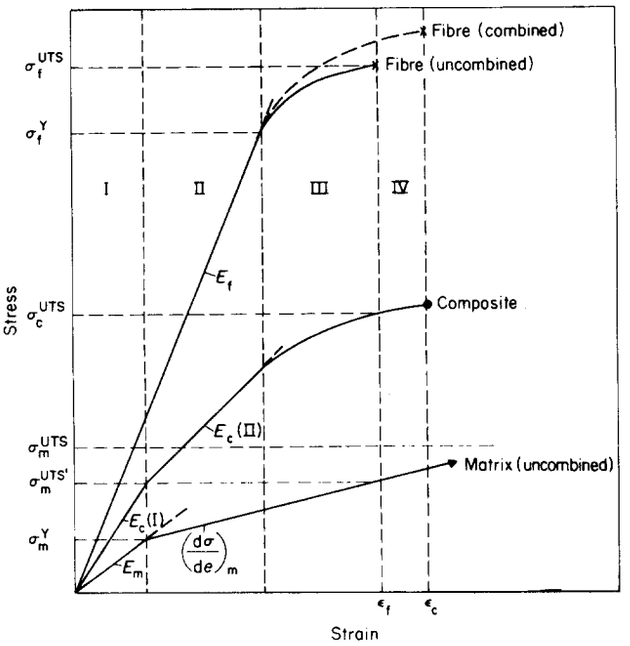

Fig. 11 Schematic representation of the stress–strain behaviour of continuous fibre, metal matrix composites

1. Fibres and matrix deform elastically
2. Matrix deforms plastically, fibres elastically
3. Fibres and matrix deform plastically
4. Fracture of the composite.

In stage 1, the composite Young's modulus E_c is given by

$$E_c = E_f V_f + E_m(1 - V_f)$$

where E_f, E_m = moduli of the uncombined fibre and matrix, respectively, and V_f = volume fraction of fibres. Composites for structural applications use high modulus filaments to improve the elastic properties; however, since the modulus of Nb-Ti is lower than that of copper (~ 8.2 compared to $\sim 11.7 \times 10^{10}$ N m^{-2}), composites of these materials exhibit unique behaviour in that the modulus of the composite is lower than that of the matrix.

In stage 2 a 'secondary Young's modulus' is defined by $E_c = E_f \times V_f + (\partial\sigma/\partial\epsilon)_m \times (1 - V_f)$ where $(\partial\sigma/\partial\epsilon)_m$ = slope of the matrix stress–strain curve in the uncombined state at a strain level in stage 2. The ultimate tensile strength of the composite σ_c is given by $\sigma_f = \sigma_f V_f + \sigma'_m(1 - V_g)$, where σ_f is the ultimate strength of the fibres and σ'_m is the stress in the matrix when the fibres are strained to their ultimate tensile strain.[54] Stages 1 and 2 are of most interest for superconducting applications, and in particular stage 2 which produces a 'pseudoelastic' effect phenomenologically similar to the effect already discussed. If a composite is loaded into stage 2 and then unloaded, the fibres (still elastic) will contract and place the matrix into compression. The fibres will show a residual tension on unloading to a macroscopic stress of zero. Therefore, a hysteretic loop will be obtained under the above stress cycle. Several assumptions listed above for the rule of mixtures do not hold for multifilamentary Nb-Ti/Cu, Al composites. In most composites the fibres are twisted into a helical configuration. The case of fibres aligned to varying angles from the tensile (composite) axis has been treated both theoretically[57] and experimentally.[58] The composite

tensile strength drops off rapidly with angle between the aligned continuous fibres and the tensile axis.[58] A marked reduction in tensile strength (~ 50%) was observed in a silica fibre/aluminium matrix composite when the above angle approached ~ 10°. However, Heim[59] has calculated the effects of twisted filaments considering the stress distribution of Nb-Ti filaments over the wire cross-section with respect to axial strain. For an assumed conductor geometry and with a copper to superconductor ratio of 4/1, filament diameter = 0.5 mm, 84 filaments, and twist pitch of ~ 80 per m (2 per in) he obtains ~ 6% correction factor from the case where twist is ignored. He proposes that appropriate analyses can thus be made by using Young's modulus which is 0.94E of Nb-Ti in the above case.

The rule-of-mixtures also assumes that the composite components are not in a state of residual stress before testing. Heim[59] has also shown that the typical wire manufacturing process can leave both the filament and matrix with large residual stresses. Thus the details of final thermomechanical processing as well as stresses generated by the differential thermal contraction of the NbTi and Cu (~ 1:2) during cooling can complicate the assumed stress distribution in the composite.

In spite of the complexities in superconducting composites described above, the stress–strain data generated so far agree fairly well with the rule-of-mixtures. Easton and Koch[9] found values for Young's modulus that obeyed the rule-of-mixtures to within experimental error for a variety of multifilamentary conductors. While values for ultimate tensile strength did not show such simple agreement, they also approximated rule-of-mixture behaviour (see Fig. 12). The temperature dependence of the composite and component stress–strain curves is illustrated by comparing room temperature measurements data (Fig. 13) with measurements taken at 4.2 K (Fig. 14). At ambient temperature, the composite behaves as predicted. The higher values of ultimate tensile strength and elongation of a composite at strains greater than the fracture strain of the filament have been attributed[60] to a restraint by the matrix on localized necking of the filaments. Thus the filaments in a composite can show increased elongation compared with individual wires where necking occurs at low strain values. since fracture follows necking with little further uniform deformation.

At 4.2 K (Fig. 14) the situation is markedly different. Here the Nb-Ti filament shows greater apparent elongation than the composite. However, some of this elongation is not permanent plastic deformation, but results from the reversible pseudoelastic behaviour already discussed.

Most (or all) of the observed plastic deformation occurs with the discontinuous load drops. If these load drops are due to mechanical twinning or to an elastic martensitic phase transformation the resulting shape deformation as surface 'kinks' may be prevented by the matrix, thus preferentially introducing fracture. Serrations are often observed in the composite stress–strain curve at 4.2 K, although not to the extent seen in the Nb-Ti filaments. This is further indirect evidence for the constraining effects of the matrix on the deformation mode in the filaments at 4.2 K.

Verkin et al[34] made stress–strain measurements at 300, 77, 22, and 4.2 K on composite cables of 0.17 mm diameter Nb-Ti filaments clad with copper and placed six to a cable of 0.82 mm od. Ultimate tensile strength and percent elongation values agree almost exactly with data of Easton and Koch[17] on a conductor with similar copper to superconductor ratio (~ 2.8 : 1). Verkin et al also observed serrations in the stress–strain curves at 4.2 K.

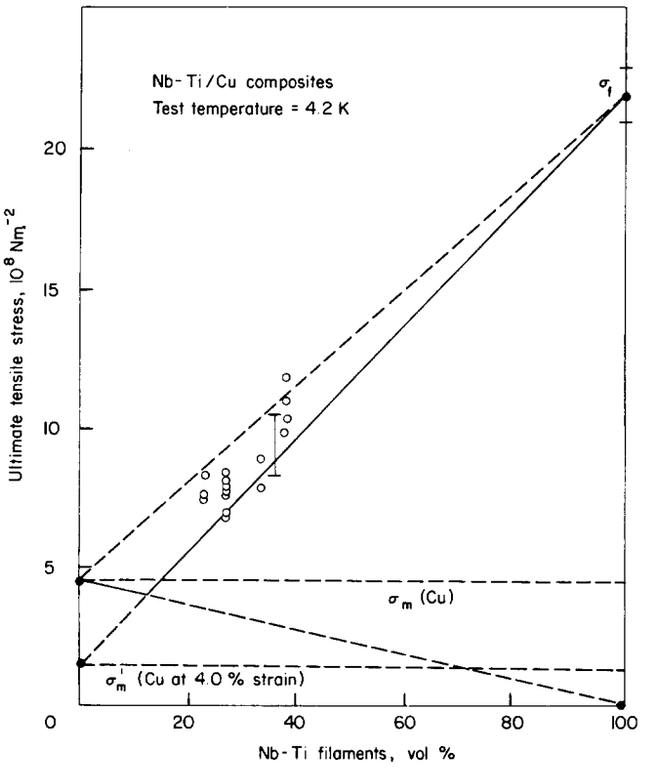

Fig. 12 Relationship between ultimate tensile strength and volume % of Nb-Ti filaments in a copper matrix

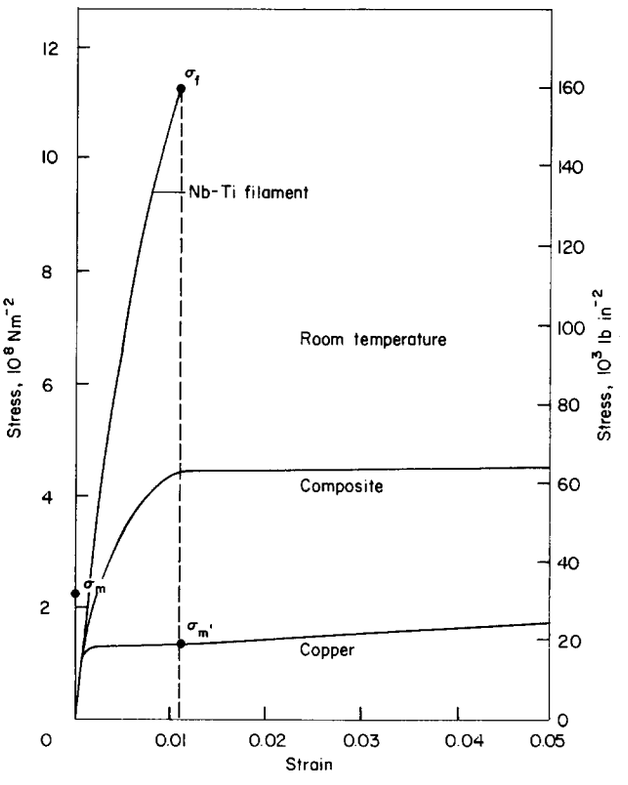

Fig. 13 Room temperature stress–strain curves of matrix, filament, and composite for a 2.8:1 Nb-Ti/copper composite

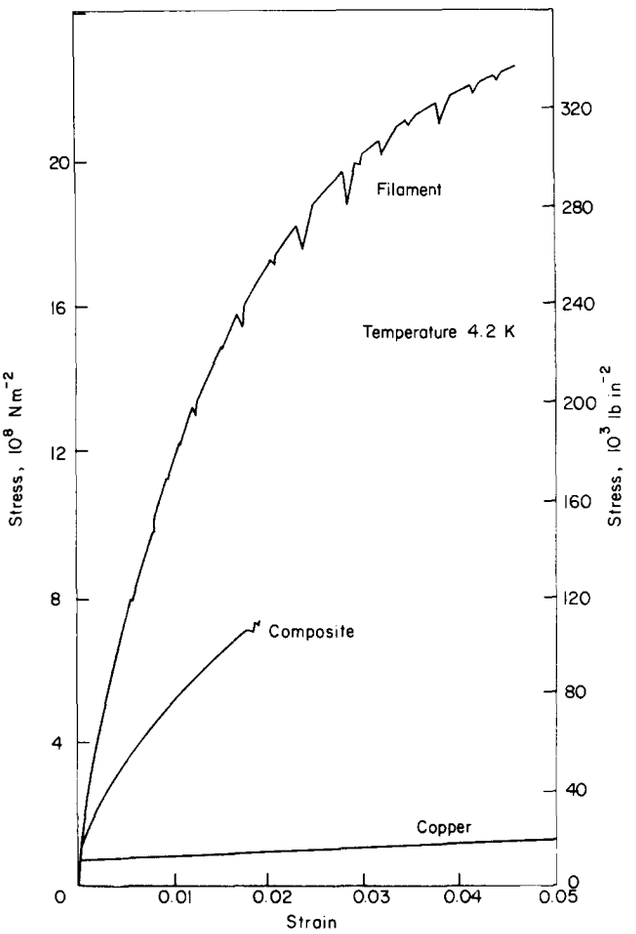

Fig. 14 4.2 K stress–strain curves of matrix, filament, and composite for a 2.8:1 Nb-Ti/copper composite

Hillman[30] presented room-temperature mechanical properties data on Nb-Ti/Cu composites with 61 or 120 filaments per conductor as well as several single core conductors. The volume fraction of superconductor in the composites varied from 16 to 50%. He finds larger values for the fracture stress than would be predicted by the rule of mixtures. He cites several factors which complicate this simple rule including the stress state and the nature of the bond between superconductor and matrix.

Reed et al[5] measured the tensile properties of a multifilamentary Nb-Ti/Cu composite and its components at 298, 77, and 4.2 K. The Young's moduli of the components were lower than values for bulk samples, but the rule-of-mixtures was well obeyed for the components and composite. Values of the composite tensile strength predicted by the rule-of-mixtures fell about 25% below the measured composite values. This was rationalized by assuming that the copper in the composite was in a more work-hardened condition than the copper wire used for comparison. Serrations were not observed at any test temperature down to 4.2 K. (Subsequent work[36] by the NBS Boulder Group did report serrated stress–strain curves at 4.2 K in Nb-Ti composites.) This group found the yield strength to increase slightly and the percent elongation at fracture to decrease with increasing strain rate at 4.2 K. Hysteresis in stress–strain cycles was observed with anelastic recovery effects increasing with increasing applied stress.

Fisher et al[61] studied the influence of cyclic stresses at 4.2 K on transport properties of superconducting composites. The samples were constant-strain cycled in pure tension-compression modes to strains of the order of 0.1 to 0.5% and up to ~ 2000 cycles. Most of this work involved measurements of changes in resistivity and critical current density and will be reviewed in the section on the effects of stress. However, measurements of the current indicated that filament fracture occurred with a tension strain of 0.5% at 565 cycles.

The Bauschinger effect has been invoked[59] to describe the inelastic behaviour of superconducting composites. The Bauschinger effect describes the experimental observation that the elastic limit in compression is reduced following tensile prestrain. For Nb-Ti/Cu composites in stage 2 of the stress–strain curve, the copper yields in tension. During unloading, the constraint of the still elastic fibres places the copper in compression. A hysteresis loop is generated according to the simplified composite analysis presented above. The Bauschinger effect determines the shape of the loop however. Heim[59] claimed his composites were in a residual stress state due to the manufacturing process such that the precompression of the copper decreased the copper elastic limit to essentially zero before testing. Easton and Koch[9] have found, however, in many multifilamentary composites a clearly defined elastic region (stage 1) from which good Young's moduli can be obtained. The final processing steps must be critical in this regard. After repeated stress cycling around a hysteresis loop, both Heim and Easton find no significant change in loop character with further cycling. The 'stabilization' (that is, closure of hysteresis loops) has been observed in other composite systems such as W-Cu[62] after several strain cycles into stage 2. The dislocation dynamics and microstructure of the Nb-Ti/Cu composite (matrix) requires further investigation for a clear picture of the microscopic mechanism responsible for the stress–strain hysteresis loops.

Mechanical behaviour of compound superconductors

The compound superconductors to be considered in this review are the high field A-15 materials (Nb_3Sn, V_3Ga, Nb_3Ge, etc), the refractory metal nitrides and carbonitrides [NbN, Nb(CN)], and the Laves phases V_2(Hf, Zr). One consistent feature of all superconducting compounds at ambient and lower temperatures is their inherent brittleness. Thus, unlike the alloys already discussed little information on plastic properties is available so most of the mechanical behaviour to be discussed will involve elastic properties and composite performance.

Elastic properties of compound superconductors

Compounds with the A-15 crystal structure. Because of their potential technological importance as high field superconductors and the fascinating 'anomalous' elastic behaviour and structural instabilities observed in them the elastic properties of A-15 superconductors have been extensively studied. No attempt will be made here to review the vast literature on the subject, particularly since the reader may be referred to several recent and comprehensive review papers in this area.[63–65] L.R. Testardi sums up the situation . . . 'indeed, as a class and as a phenomenon there are few materials for which so much detailed information is now available.'[64] However, we will briefly outline some of the

major experimental observations which bear on the stress effects in these superconductors to be discussed later. Most of the elasticity and structural studies have been carried out on either V_3Si or Nb_3Sn due primarily to the availability of single crystals of these materials. Ultrasonic experiments in both V_3Si[66] and Nb_3Sn[67] revealed anomalous, though differing, elastic constant dependence on temperature. Unlike most materials (for example, Nb-Ti) which show a stiffening of the lattice on cooling, V_3Si and Nb_3Sn exhibit a lattice softening as evidenced by a near vanishing of the elastic (shear) moduli $(C_{11} - C_{12})/2$ as the temperature is decreased from ambient to a low critical temperature. In V_3Si the decrease in $(C_{11} - C_{12})/2$ is stabilized to a low constant value at either T_c(~ 17 K) or, in samples which undergo a martensitic phase transformation, there is an arrest at the structural transformation temperature T_m(~ 21 K).[66] In Nb_3Sn $(C_{11} - C_{12})/2$ also decreases to a low value with decreasing temperature but at T_m(~ 43 K) rises again to a high stable value below T_m.[67] The reasons for these differences are not at present understood.

The structural changes are martensitic transformations from the cubic A-15 crystal structure to a tetragonal structure. The tetragonal distortions are small; for V_3Sn, $c/a \approx 1.0024$ (T_m = 18–25 K);[68] for Nb_3Sn, $c/a \approx 0.9936$–0.9964 ($T_m \approx$ 43 K). The martensitic transformation results in a twin related domain structure in the tetragonal state which gives rise to a shape deformation of the sample surface similar to that observed in other martensitic transformations. Martensitic transformations have also been observed in V_3Ga[70] and $Nb_3Al_{0.75}Ge_{0.25}$.[71] The transformations are not observed in all samples of a given material.[68] The occurence of the transformation has been related to a defect structure and it has been reported[64,68] that non-transforming V_3Si samples have lower resistivity ratios, $\rho(200\text{ K})/\rho(20\text{ K}) \approx 10$–$20$, compared to values of ≈ 40–80 for transforming samples. This has recently been rationalized[72] by assuming that point defects give rise to microdomains of tetragonal distortions which stiffen the cubic lattice for shear-type motion and stabilize the cubic phase.

One would expect the mechanical stress to affect the above structure-sensitive phenomena, and this is the case. Uniaxial stress (~ 2×10^7 N m^{-2}) along [001] directions in single crystal V_3Si caused a change in the morphology of the domains of the tetragonal phase.[73] The domains rotate such that the a_0 axis in each is parallel to the applied stress. Stress did not change T_m (to a resolution of 0.1 K) but reduced the volume fraction of tetragonal phase present. At high stress values (~ 3.0×10^7 N m^{-2}), the transformation was totally suppressed. At this stress level the strain is ~ 10^{-3}, comparable to the strain produced during transformation without applied stress. Thus, an applied strain similar in size to the transformation strain suppresses the transformation.

The elastic moduli in V_3Si increase with stress as measured in uniaxial tension[74] or by ultrasonic experiments.[64] The tetragonal distortion given to the crystals by the applied strain stabilizes the cubic phase and the attendant phase stability increases the shear modulus over the unstrained condition by a factor of 2.

While most of the experiments on elastic behaviour and structural stability in A-15 superconductors have been carried out on single crystals, the elastic constant softening[75,76] and structural transformations[76,77] have been

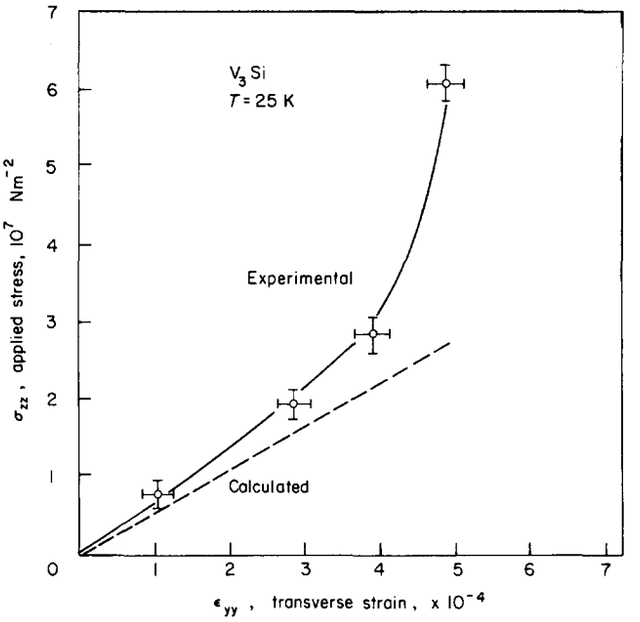

Fig. 15 Non-linear stress–strain behaviour of a V_3Si single crystal under uniaxial compression in the (001) direction at 25 K (after Patel and Batterman[73])

observed in a variety of polycrystalline materials. Old and Charlesworth measured Young's modulus of bulk Nb_3Sn by an ultrasonic technique and found it to be 17.9×10^{10} N m^{-2} at room temperature.[78]

Hydrostatic pressure also influences the elastic moduli. At room temperature the bulk modulus and the shear moduli, C_{44} and $(C_{11} - C_{12})/2$, increase with hydrostatic pressure[79] in V_3Si. Below ~ 80 K the shear modulus (which is responsible for the instability) decreased under pressure. In non-transforming samples the negative pressure dependence reaches a maximum value at T = 15–20 K and then remains approximately constant. In a transforming sample the pressure dependence became positive again at ~ 50 K, no measurements were made below 37 K. Hydrostatic pressure decreases T_m in V_3Si by 1.5×10^{-4} kbar (10^5 N m^{-2}).[80] Recent studies[81,82] of V_3Si under hydrostatic pressure at room temperature indicate that in addition to the contraction of the unit cell, changes of a structural or defect changes may occur.

Anharmonic effects are observed in A-15 materials. Patel and Batterman,[74] using an x-ray diffraction technique, found a non-linear stress–strain relationship for a V_3Si single crystal under uniaxial compression in the [001] direction. The relationships between the applied stress, σ_{zz} and the measured transverse strain, ϵ_{yy}, is illustrated in Fig. 15 for a sample tested at 25 K ($T > T_m$). The results imply that the crystal is stiffer at higher stresses. Below the transformation temperature T_m, the reorientation of the tetragonal twin domains under stress provides a possible source for pseudo-elastic behaviour. Recently, anharmonicity was investigated by Smith et al[83,84] in V_3Si and Nb_3Sn by measurements of thermal expansion. In V_3Si samples, with 25 and 26 at % Si, a large, anomalous, negative thermal expansion coefficient was observed below ~ 60 K. An anomalous positive thermal expansion coefficient was seen in a transformed Nb_3Sn sample below T_m(~ 43 K) but no anomalous behaviour was noted in a non-transforming sample.

Elastic behaviour of other compound superconductors. In contrast to the A-15 superconductors, elastic property data is limited for other compound superconductors. Lattice instabilities occur in the C-15 superconductors (Laves phases). Lawson and Zachariasen[85] report a cubic to orthorhombic transformation starting at ~ 120 K in HfV_2 while Moncton[86] found a cubic to rhombohedral transformation in ZrV_2, also at ~ 120 K. This is a curious result, since the pseudobinary alloys $Hf_xZ_{1-x}V_2$ form complete solid solutions at ambient and higher temperatures in the C-15 phase. These pseudobinaries are potentially useful superconductors due to their high values of H_{c2} (~ 23 T at $X = 0.5$). Finlayson et al[87] have made internal friction measurements in both HfV_2 and ZrV_2 and find large peaks which they tentatively attribute to mechanical effects such as phase boundary or defect motion at temperatures below the phase transition. Doherty and Gibbons[88] previously observed a similar effect in ZrV_2 but at higher temperatures (peak ~ 120 K).

The B-1 superconductors [NbN, NbC, Nb(CN)] are of interest because of their high transition temperatures (to 18 K) and H_{c2} (15 to 20 T) values. The Young's moduli for these materials are expected to be high. The room temperature modulus for NbC is 48.8×10^{10} N m^{-2}.[89] Techniques have been developed for producing NbC and Nb(CN) superconductors on carbon fibres by chemical vapour deposition.[90,91] The high strength and modulus of the carbon fibre substrates are expected to provide desirable mechanical properties. These materials will be discussed further.

Plastic behaviour of compound superconductors

All the potentially useful superconducting compounds are brittle at ambient and lower temperatures and fracture occurs in the elastic strain regime. Thus, fracture tensile strains of ~ 0.1–0.3% are typically observed. While speculation as to the relative ductility of the various A-15 compounds has been common, no systematic comparison has been made to our knowledge. In fact, such a comparison would be difficult since fracture strain in the elastic regime is sensitive to surface flaws, cracks, and sample alignment, which causes a scatter in the data that might mask any trend between these apparently brittle materials. The brittleness in these compounds is presumably from the difficulty of dislocation motion at and below room temperature. This in turn is generally believed due to the nature of bonding in the compounds which must be either directional (covalent) or reflect the high degree of long range order. However, at high temperatures (relative to the melting temperature) plastic behaviour can be observed in brittle compounds. Levinstein et al[92] plastically deformed V_3Si single crystals at 1520°C and studied the dislocation structure by etch-pitting techniques. The observation of dislocation arrangements suggested that the slip system in V_3Si is {100} <001>.

When the $Hf_xZr_{1-x}V_2$ C-15 phases were first found to be high field superconductors it was suggested[93] that they might have desirable mechanical properties due to their lower microhardness values (~ 270–450 kg mm^{-2}) compared with those of A-15 compounds (~ 1000 kg mm^{-2}). This assumption of possible 'better ductility' has been subsequently repeated.[94] We find no evidence for such a conclusion; rather we found the $Hf_xZr_{1-x}V_2$ C-15 phases to be brittle.at ambient temperatures, as are other C-15 phases. There is not necessarily a one-to-one correlation between hardness and ductility – many 'soft' materials are completely brittle. 'Hardness' is a complex quantity controlled by bonding while ductility reflects the ability for dislocation motion to occur.

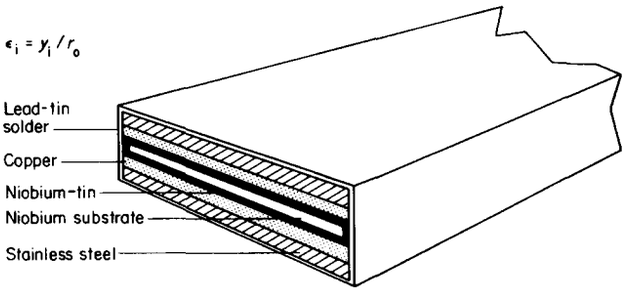

Fig. 16 Schematic illustration of a typical Nb_3Sn tape composite (after Benz[99])

Mechanical behaviour of composite compound superconductors

Besides the necessity to combine high conductivity normal material with the superconductor for stability purposes, it is mandatory to prepare the brittle compound superconductors in composite form in order to handle them. The first Nb_3Sn conductors developed at Bell Telephone Laboratories in the early 1960s[95,96] were made by packing a mixture of Nb and Sn powder in a Nb tube and drawing the composite down to wire. Solenoids were wound from the wire and then reacted to form the Nb_3Sn phase.

Problems with brittleness and porosity of the wire formed in this manner led to the development of flexible tape conductors that were reacted prior to winding. These tapes were made either by chemical vapour deposition[97] or diffusion of Sn into a Nb substrate.[95] Copper or aluminium as well as strengtheners such as stainless steel were laminated with solder to the tape conductors. Benz[99,100] has described and analysed the mechanical behaviour of diffusion processed Nb_3Sn-copper stainless steel tapes. A typical symmetrical tape composite is illustrated in Fig. 16.

A large compressive stress develops in the Nb_3Sn layer as the composite is cooled from the bonding temperature (353 K) to the operating temperature (4.2 K) because the thermal expansion coefficients of the copper and stainless steel are much larger than for Nb_3Sn. Thus, an external tensile force applied to the composite at 4.2 K can reach substantial values before the stress on the Nb_3Sn changes from compressive to tensile. The stress where this occurs has been defined as the 'design stress level' and given as a safe operating stress. The average stress on the total conductor which causes fracture of the Nb_3Sn was defined as the failure stress. Elastic behaviour is assumed in the Nb_3Sn up to failure.

Bending also causes strain. For a radius of curvature r_0, mechanical strain ϵ_i is equal to y_i/r_0 where y_i is the distance from the neutral axis of bending. If t_{Nb_3Sn} is defined as the thickness of the Nb + Nb_3S central layers, then $\epsilon_i = t_{Nb_3Sn}/2r_0$. If the fracture ductility in tension of Nb_3Sn is $\sim 0.2\%$, bends around a radius less than 250 times t_{Nb_3Sn} will initiate fracture in the outer layers of Nb_3Sn. Non-symmetric composites can also be analysed in the same manner with the Nb_3Sn layer kept at the neutral axis by balancing the thicknesses of the composite layers;

that is, $E_{Cu}t_{Cu} = E_{ss}t_{ss}$ where E_{Cu}, E_{ss} are the moduli of copper and stainless steel and t_{Cu}, t_{ss} are the layer thicknesses. Benz found failure stresses to be higher than the calculated values.[100] In an analysis of Nb_3Sn – aluminium-stainless steel composites, Henning et al[101] found that while bare Nb_3Sn fractures at ~0.2%, the fracture strain of the Nb_3Sn in the composite increases to ~0.3%. They claimed that this was due to the initial biaxial compressive stresses producing lateral constraints on the Nb_3Sn. Using the above definitions, Henning et al,[101] Benz,[100] and the Brookhaven Group[102] found the experimentally measured failure stresses had identical or higher values than predicted values. The few instances when the measured values were lower were attributed to prior damage due to handling of the composite.

In recent years Nb_3Sn[103] and V_3Ga[104-106] have been produced in multifilamentary form by variations of the 'bronze' method whereby Nb (or V) rods are inserted into a Cu-Sn (Cu-Ga) matrix and co-deformed to fine twisted filaments as in the Nb-Ti composites already discussed. The composites are then given a reaction heat treatment to form Nb_3Sn (or V_3Ga). The composite behaviour outlined in the section on the mechanical behaviour of composite bcc superconductors should also apply to these multifilamentary materials with additional complications due to the extreme brittleness of the A-15 compound layer and the presence of an unreacted Nb (or V) core. Tensile data on these materials has only recently become available. Old and Charlesworth[78] made room temperature tensile tests on multifilamentary Nb_3Sn prepared by the bronze method with the number of filaments ranging from 37 to 5143, with nearly total and partially reacted Nb, and with initial Nb volume fractions in the bronze from 11% to 25%.

Two markedly different types of stress–strain curves were observed in these materials (Fig. 17). In curve A the composite exhibits elastic behaviour up to ~0.15% strain where yielding occurs. The wire then deforms plastically until fracture occurs at total strains between 0.5 and 0.8%. In type B behaviour, the yielding at 0.15% strain was followed by a plastic region up to 0.9% strain. Further deformation then continued at an essentially constant load until fracture at ~10% strain.

Attempts to use the simple law of mixtures criteria failed to explain this behaviour. However, it was found that samples containing 16% or more Nb (before reaction) followed type A behaviour and those with less than 15% exhibited type B stress–strain curves. Optical metallography revealed localized transverse cracks in type B samples at strains ~0.9%. In type A samples cracks spread across the sample and failure occured whereas, in type B samples the damaged regions increased with strain until the entire length of the wire was cracked at fracture. Acoustic emission studies indicated that cracking started at ~0.7% strain. This is much higher than the ~0.2% fracture strain in bare Nb_3Sn, and, if accurate, may be due to the complex stress state in the filaments. However, Vandervoort[107] also studied room temperature deformation in a multifilamentary Nb_3Sn conductor with acoustic emission and reported some filaments fracture prior to the 0.2% strain level, and nearly all the filaments fractured by 1.6% strain. A compressive stress–strain curve also indicated initial filament fracture at ~0.2% strain and buckling with a majority of the filaments fractured at 0.6% strain. At present we are not able to judge whether the differences in Old and Charlesworth's or Vandervoort's data

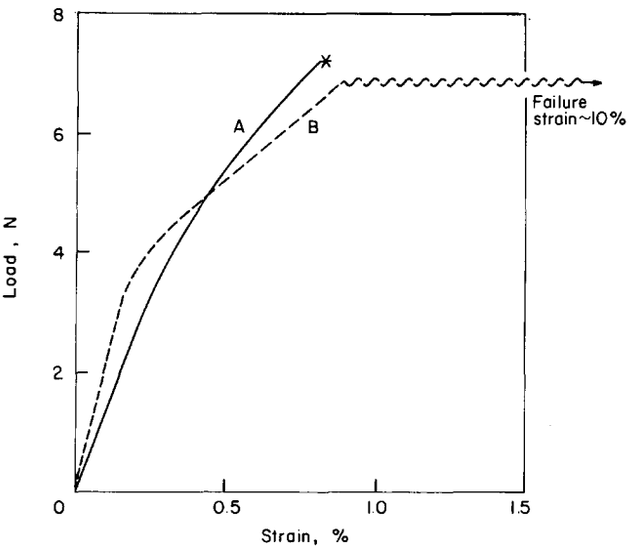

Fig. 17 Two types of room temperature stress–strain behaviour in Nb_3Sn multifilamentary composites
a– > 16% Nb; b– < 15% Nb; (after Old and Charlesworth[78])

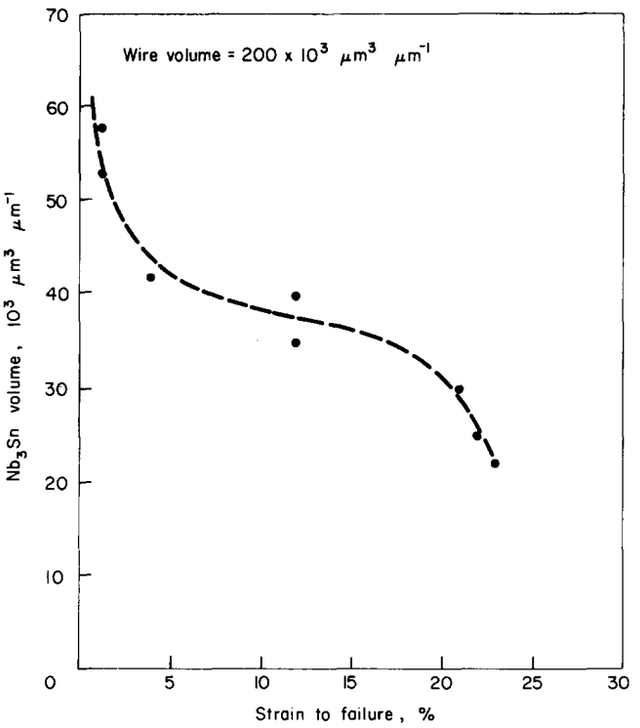

Fig. 18 Fracture strain in Nb_3Sn multifilamentary composites as a function of volume of compound (after McDougall[108])

reside in real material differences or in the sensitivity and/or interpretation of the acoustic emission data.

McDougall[108] made tensile measurements on multifilamentary Nb_3Sn at room temperature and at 4.2 K. The reaction temperatures and times were varied to give Nb_3Sn layers ranging from ~11 to 28% of the wire volume. The critical strain for failure decreased with increasing volume of compound. A volume of ~20% separated samples with high strains to failure from those with low fracture strains (see Fig. 18). This behaviour is characteristic of composites in which brittle interfacial layers separate ductile filaments from a matrix. The failure of the Nb_3Sn layer was analysed

in terms of interface separation caused by plastic deformation of the bronze matrix and niobium core. Any interface separation acts as a stress concentrator (notch) and induces fracture in the compound. It is unlikely that the proposed fracture model is necessary to explain cracking in the inherently brittle Nb_3Sn. The nature of the stress distribution within the Nb_3Sn layers is probably the determining factor. However, McDougall shows that increased compound thickness reduces the critical strain to failure for single repeated stress of the composite. He finds the stress–strain curves at room temperature to have the inflexions noted above. A doubly inflected stress–strain curve was observed at 4.2 K and is interpreted as due to an increase in the Nb modulus relative to the bronze.

Larbalestier et al[109] have made tensile measurements at 4.2 K on a commercial multifilamentary Nb_3Sn composite (3780 filaments) consisting of 11 volume % Nb before reaction. Various reaction treatments in the temperature range 665–780°C were given. No two samples had identical stress–strain curves but the following general features were observed. The proportional limit occurred at ~ 0.1% strain and was followed by a linear stress–strain region up to 0.8–1.0% strain. Failure strains ranged from 4.6 to 13.8%. Cracks were observed by metallographic techniques at strains less than 1.0%; however, most of them did not penetrate the Nb core. There was a large variation in initial elastic modulus (5.5 to 25.5 x 10^{10} N m^{-2}).

Easton[10] has observed stress–strain behaviour at 4.2 K in commercial multifilamentary Nb_3Sn composite conductors similar to the above examples which exhibited large strains to failure (~ 10%). Ultimate tensile strength was 4.2 x 10^8 N m^{-2} and Young's modulus for this composite was 16.2 x 10^{10} N m^{-2}.

Thus, it appears that although most commercial materials exhibit extensive strain before fracture (type B behaviour of Old and Charlesworth), cracking of the Nb_3Sn layers occurs at low values of strain (~ 0.2–0.7%).

A unique class of multifilamentary A-15 superconductors has been developed by Tsuei and co-workers.[110] These copper-base alloys were prepared by casting followed by cold-work and reaction heat treatment. This procedure forms discontinuous filaments of Nb_3Sn in a bronze matrix – typically ~ 15% of the volume consisting of Nb-Nb_3Sn filaments. No tensile data are available on these conductors but bend tests showed no degradation in superconducting properties and the mechanical properties are expected to be dominated by the behaviour of the matrix.

Tanaka and Furuto[111] made room temperature tensile tests on multifilamentary V_3Ga composites. They observed an elastic limit at ~ 0.08 to 0.1% strain and a second inflexion in the stress–strain curve at 0.9–1.1% strain. Fracture strain was not reported. Scanning electron microscopy revealed cracking in the V_3Ga filaments after a bending strain of 0.8%.

Composites of Nb(CN) chemically vapour deposited on high strength carbon fibres are being developed as superconducting materials.[91] Preliminary tensile data[112] on such composites are presented in Table 3.

Effect of stress on superconducting properties

Effects of stress on the superconducting properties of alloy superconductors

The influence of mechanical stress on superconducting properties can assume several forms and levels of importance. The defects (dislocations, point defects, stacking faults) created by plastically deforming superconductors influence superconducting properties to varying degrees. The transition temperature (T_c) and the thermodynamic critical field (H_c) can be slightly altered by internal stresses which may change the electronic structure of phonon spectrum.[113] In most cases such changes are small – a few tenths of a degree at most. Thermodynamic treatments of stress effects have been applied to specific elements with some success but only recently[114] has a theory been developed which *semi-quantitatively* predicts the pressure dependence of T_c in the transition metals. Substantial changes in T_c can occur with stress if a stress-induced phase transformation takes place.[115]

Finlayson and Milne[116] found unusually large effects of plastic deformation on T_c of a Nb–32 at % Zr alloy cold-rolled at room temperature. The transition temperature increased steadily with deformation; a maximum increase of 0.5 K at 93% reduction in area. Similar deformations in Nb-Ti alloys and pure niobium did not produce such shifts in T_c. This result is still not explained, but the authors suggested the possibility of a low temperature phase transition promoted by the internal strains, or a change in the phonon or electronic spectrum due to the defect structure.

The upper critical field, H_{c_2}, depends upon an 'intrinsic' contribution, consisting of those electronic and phonon parameters which influence T_c, and an 'extrinsic' contribution which depends upon electron mean free path and is thus proportional to normal state resistivity. To the extent that normal state resistivity is increased by mechanical deformation, H_{c_2} would be raised. However, in concentrated alloy superconductors such as Nb-Ti and Nb-Zr, the resistivity is sufficiently high that even severe cold deformation does not increase H_{c_2} dramatically and therefore is of little practical significance.

The critical current density, J_c, is the most structure-sensitive superconducting parameter since it depends on the

Table 3. Tensile data for carbon and niobium carbonitride fibres

Sample	UTS (N m^{-2})		Fracture strain
	300 K	4.2 K	4.2 K
Carbon fibres (Thornel 300)	16.2 x 10^8	15.8 x 10^8	4.9%
Coated with Nb $N_{0.58}C_{0.41}$	7.9 x 10^8	4.1 x 10^8	1.5%

interaction between the fluxoid lattice and crystal defects. The introduction of a fine dislocation cell structure by heavy cold deformation is one of the major factors in producing high values of J_c in commercial superconductors. The role of defects created by mechanical stress in increasing J_c, and the fluxoid pinning problem in general has been treated extensively in a number of reviews (for example, reference 117) and will not be discussed here. Similarly, the influence of the superconducting state on deformation mechanisms has been previously reviewed[118] and will not be presented here.

We are mainly concerned with the effect of stress on $J_c(H)$ under operating conditions, that is, at 4.2 K. To determine this effect requires the simultaneous measurement of J_c in a magnetic field under controlled stress–strain conditions at the temperature of liquid helium. Equipment for such measurements has only become available in recent years and the number of such experiments reported is limited. Ekin et al [119] measured the effect of stress on J_c in a NbTi/Cu (1/1.8) composite wire containing 180 filaments at 4.2 K in transverse magnetic fields to 8 T. A definite degradation of critical current with stress was observed which was first evident at stresses equal to ~ 1/3 the fracture stress. There was ~ 15–20% decrease in critical current at 3/4 of the fracture stress. A large part of the degradation was recoverable on stress removal as indicated by the dashed curves in Fig. 19. The percentage degradation at a given stress showed only a slight (for example, at the 80 kOe the degradation was ~ 4% greater than at 1 kOe) dependence on magnetic field.

Easton[120] has made J_c (stress) measurements on a wide variety of commercial NbTi composites at 4.2 K in magnetic fields to 7 T. The critical current density, J_c, was defined as an equivalent sample resistivity of $1 \times 10^{-11}\ \Omega$ cm and referred to the entire conductor cross-sectional area. Critical current density was reduced with stress–strain (Fig. 20). With the exception of a composite with an aluminium alloy matrix (75–21–L), the degradation in J_c was < 15% at strains to 2.0%. The Al-alloy matrix sample showed degradation of ~ 40% at 1.0% strain but Al-alloy matrix materials tested subsequent to the above measurements exhibited degradation comparable to copper matrix samples. The J_c value at zero strain was almost fully recoverable (within 1%) upon release of stress in all samples, with the exception of the Al-alloy matrix sample discussed above.

Ekin and Clark[121] have reported J_c values at 5 T on multifilamentary NbTi stabilized by high purity aluminium (RRR ≈ 5000) or OFHC copper (RRR ≈ 70). Both conductors consisted of NbTi tubes embedded in a 5056 aluminium alloy matrix with the stabilization material on the inside of the tubes. J_c decreased when the wires were given strains greater than ~ 0.5%. The degradation was almost totally reversible and did not become significant until strains of 1.5% or more were applied. The degradation of the aluminium and copper stabilized wires were identical to within 1%. The critical current was defined by three criteria; either an electric field level of 3×10^{-6} V cm^{-1} or resistivity levels of $10^{-10}\ \Omega$ cm or $10^{-11}\ \Omega$ cm (normalized to the NbTi cross-sectional area in the composite). The electric field criteria was used in most cases, but only small differences in J_c resulted from the various methods of defining J_c.

Klamut and Suenaga,[122] Ekin,[123] and Easton[120] found no influence of filament twist pitch on degradation of J_c with stress in Nb-Ti composites with copper matrices.

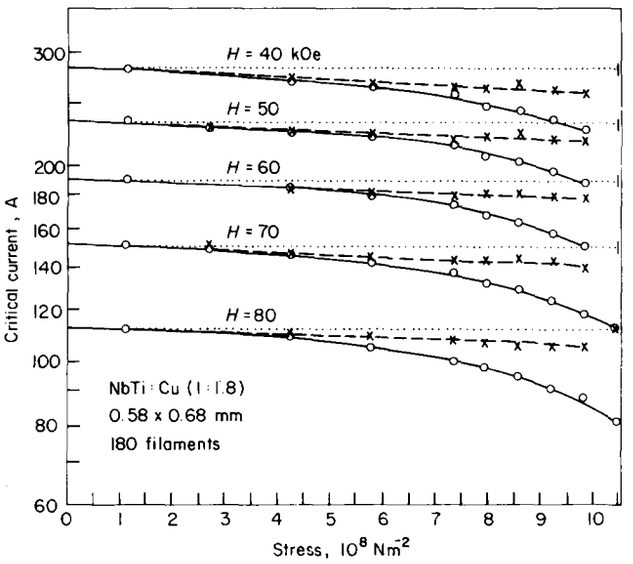

Fig. 19 Degradation in the critical current of a Nb-Ti multifilamentary composite as a function of magnetic field and stress (after Ekin et al[119])

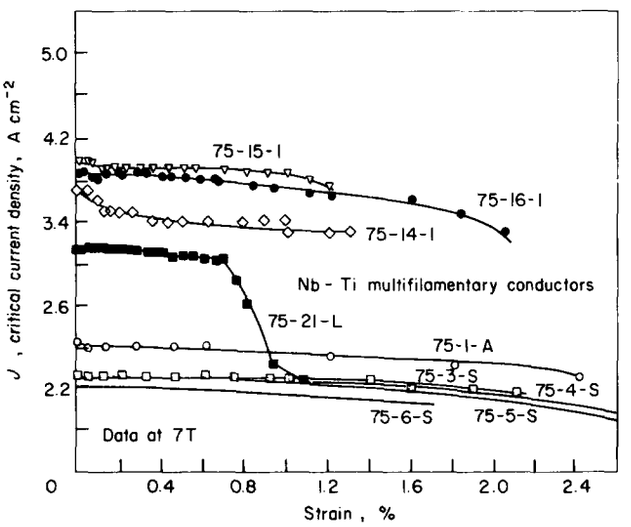

Fig. 20 The effect of strain on the critical current density of a number of Nb-Ti multifilamentary conductors

However, Easton[10] found a variation in the degradation of J_c with twist pitch in Al-alloy matrix composites (Fig. 21).

Fisher et al[61] studied cyclic strain effects on J_c in a Nb-Ti/Cu composite consisting of 18, 0.2 mm diameter filaments with a copper/superconductor ratio of 2.7. The samples which were soldered along the axis of a massive copper bar underwent constant strain cycling up to 1360 cycles. A given cycle consisted of a tensile and compressive stress which completed a stress–strain loop to a constant strain value. The changes in the unstrained critical current density at 3.94 T during the cycling schedule are illustrated in Fig. 22. In the first 200 cycles ($\epsilon_{tension}$ = 0.35%, $\epsilon_{compression}$ = 0.03%) I_c decreased ~ 3.2%. No change was noted after the next 195 cycles ($\epsilon_{tension}$ = 0.45%, $\epsilon_{compression}$ = 0.10%). The sample was then warmed to 120 K over a 20 h period and then cooled back to 4.2 K for further cycling. I_c recovered by ~ 0.1% during the warming period.

Cycling 565 times ($\epsilon_{tension}$ = 0.57%, $\epsilon_{compression}$ = 0.21%) resulted in apparent fracture of the Nb-Ti filaments. This was revealed by a linear voltage from $I = 0$ in the V–I curves as well as an increase in resistance at I_c. It was assumed this resistance was due to current sharing between the filaments and copper matrix because of the fracture.

The degradation of J_c in Nb-Ti composites by either static or cyclic stress–strain is not understood. Several possible explanations have been eliminated. The reduction in filament cross-section under strain could account for only ~ 1% of the degradation. However. any permanent dimensional changes could be responsible for the residual degradation observed on stress removal. Ekin[123] showed that the degradation could not be attributed to either a heat generation due to creep or to degradation of the matrix properties. Since the degradation is reversible the cause must be elastic or pseudoelastic. As suggested earlier, a reversible martensitic phase transformation or reversible mechanical twinning may be likely mechanisms.

Stress effects on the superconducting properties of compound superconductors

Müller and Saur[124] made the first measurements of the influence of mechanical stress–strain on T_c of the A-15 compounds. The change in T_c due to stress (torsion, bending, and uniaxial compression) was studied in tapes and wires of Nb_3Sn prepared by either the Sn diffusion process or powder metallurgy, as well as in diffusion-reacted V_3Ga. Substantial decreases in T_c were noted with $\Delta T_c \approx -1.5$ K for samples strained in torsion. Tin layers on the sample surface produced a hysteresis effect, that is, a measurable ΔT_c when stress was removed. Removal of the tin layers by etching eliminated the hysteresis in ΔT_c. Recently Pupp et al[125] studied the influence of stress produced by bending Nb_3Sn films deposited on flexible quartz substrates. An average change in T_c with tensile stress, $\Delta T_c/\Delta\sigma \approx -5 \times 10^{-4}$ K MPa^{-1} was determined. They also reassessed the results of Müller and Saur (Fig. 23). McEvoy[126] measured the stress dependence of Nb_3Sn single crystals strained in the [001] direction. He found a $-\Delta T_c$ which depended on whether or not the stress was applied above or below the martensitic phase transformation temperature T_M. This was rationalized as being due to the effect of stress on domain rotation in the tetragonal phase. Larger $-\Delta T_c$ occurred if the stress were applied above T_M. Weger et al [127] measured the effect of stress on T_c of V_3Si single crystals. They found a linear decrease in T_c with increasing compressive stress applied along the [100] direction ($-\Delta T_c \approx 0.5$ K at ~ 0.1 GPa). The change in T_c for stress applied along the [111] direction was negligible. A hydrostatic pressure of 400 atm increased T_c by 0.13 K.

Müller and Saur[128] measured changes in J_c in diffusion layers of Nb_3Sn and V_3Ga under applied stress (either tension, torsion, or bending). J_c measurements were made in fields up to 0.8 T and very large decreases (~ 2–3 orders of magnitude) were observed. It was suggested that fracture of the A-15 layers was responsible for the severe degradation in J_c.

Buehler and Levinstein[129] studied the effect of uniaxial tensile stress on T_c and J_c of Nb_3Sn-cored wire. The T_c of a Nb-sheathed wire monotonically decreased with applied stress, whereas, T_c first increased and then decreased for a Monel (Cu-Ni)-Nb-sheathed wire, as shown in Fig. 24. This

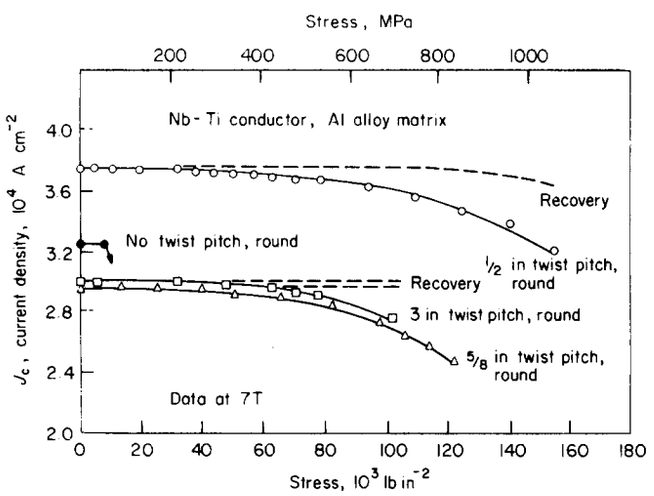

Fig. 21 The effect of stress on J_c for Nb-Ti/Al-alloy conductors with different twist pitches

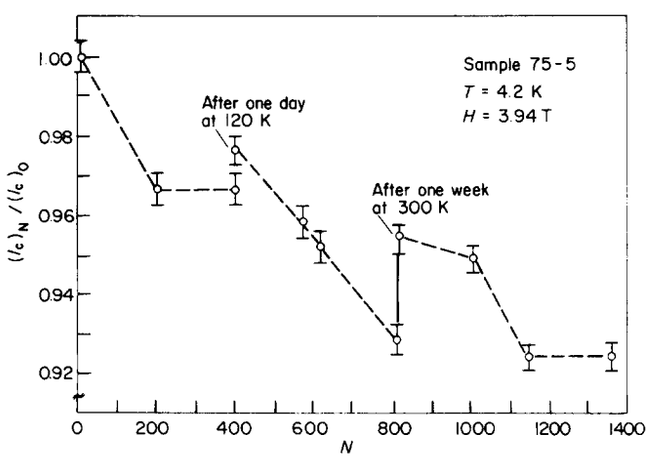

Fig. 22 The effect of cyclic stress on J_c of a Nb-Ti/Cu conductor (after Fisher etal [61])

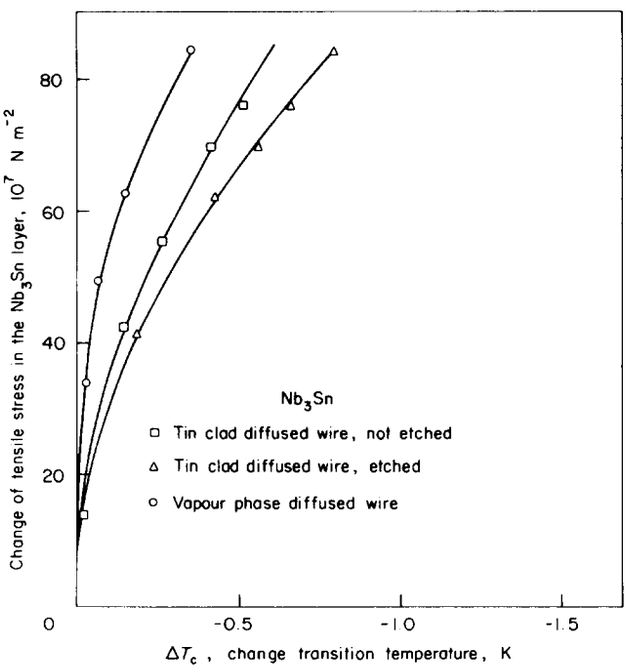

Fig. 23 Change in T_c of Nb_3Sn as a function of tensile stress (after Pupp et al[125])

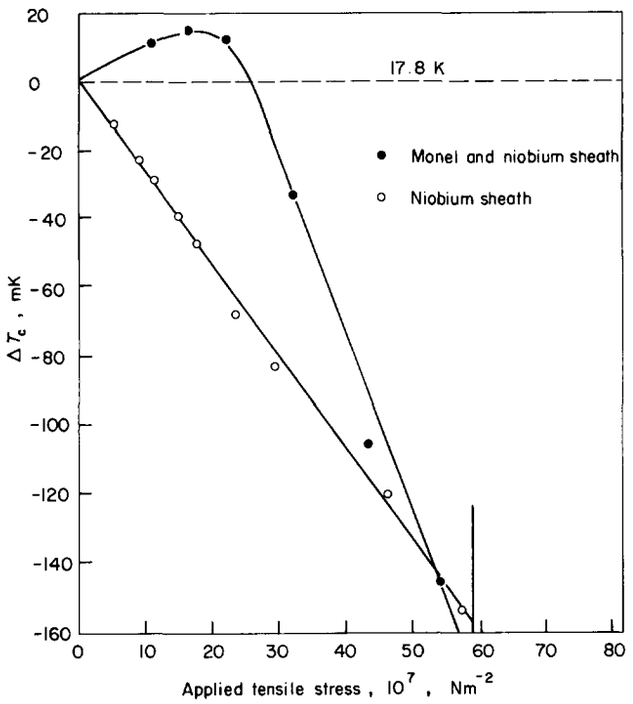

Fig. 24 The effect of applied tensile stress on T_c of Nb_3Sn wires (after Buehler and Levinstein[129])

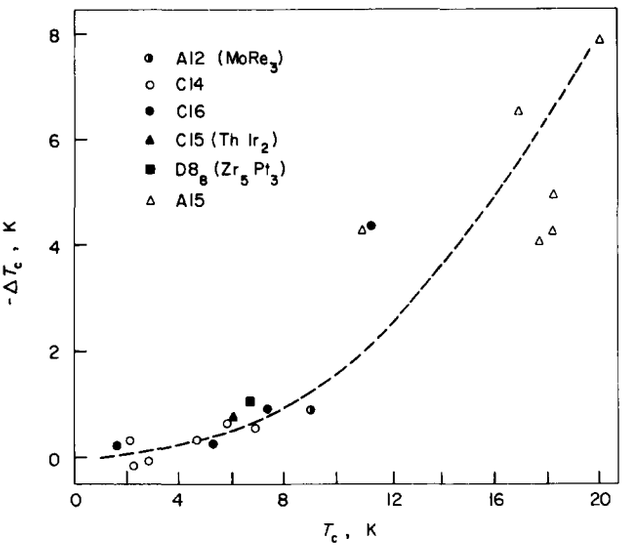

Fig. 25 The change in T_c due to stress as a function of T_c for a number of materials (after McCarthy[133])

result is explained by the Monel-sheathed wire putting the Nb_3Sn in compression when cooled to 4.2 K (due to different thermal expansion coefficients). The maximum in T_c occurs at the zero stress cross-over between compression and tension. The J_c at 8 T was found to first increase with applied tensile stress and then decrease in both the Monel and Nb sheathed samples. Complete recovery of the zero-stress J_c values were obtained for the Monel sheathed wires even after J_c was reduced by 10% under stress. Less recovery was observed in the Nb-sheathed samples.

Pulver[130] measured T_c, H_{c_2}, and J_c in V_3Si single crystals and V_3Si and Nb_3Sn diffusion wires under uniaxial tension. The values of all the critical parameters were reduced by the tensile stress. Brand and Webb[131] found that the suppression of the cubic to tetragonal transformation by uniaxial stress in V_3Si single crystals decreased J_c. Fluxoid pinning at the tetragonal-cubic phase boundaries (or internal twin boundaries) was suggested as the reason for enhanced J_c in the transformed crystals.

A second transition temperature (lower than the primary one) has been observed in pressed powders of several high T_c A-15 compounds[132] as well as a number of C-14, C-15, and A-12 superconductors.[133] ac susceptibility measurements indicate the lower T_c phase is present on the surface of the strained powders. The change in T_c is proportional to the T_c of the material, illustrated material (Fig. 25).

Smith[134] determined the hydrostatic pressure dependence of T_c in a number of A-15 compounds and reviewed the experimental and theoretical results available to him. The T_c of V_3Si and V_3Ga increase with hydrostatic pressure while T_c of Nb_3Sn and Nb_3Al decrease. None of the theoretical models for T_c explained the pressure dependence.

The 'bend test' has been the most common mechanical test for stress effects on J_c in commercial or development prototype compound superconductors. In its standard form, the superconducting tape, wire, or cable is bent around various diameter mandrels at room temperature, straightened, and then its J_c measured at 4.2 K. This test simulates any stress-induced damage which might be incurred during fabrication of a device at room temperature. In general, the bend radii for tapes which exhibit the first signs of degradation follow the simple elasticity analyses of Benz[100] and Henning et al.[101] The fracture strain for the compound (~ 0.1–0.3%) is approximately constant so that the critical bend radius depends upon the layer thickness, that is, its outer fibre's distance from the neutral axis of bending.

It has been shown[102] that if J_c measurements are made with the sample still bent at a given radius, larger critical bend radii are obtained than in the case of samples measured after straightening. This implies that some recovery takes place on straightening. However, Randall et al[135] found more reproducible behaviour in multifilamentary material if J_c were measured on the bent conductor (Fig. 26). The difference between the conductors is due to the smaller strains induced in the twisted filaments at a given bend diameter.

A characteristic of both tensile and bend data is the apparent increase in current density with stress prior to degradation. Randall et al[135] attribute this to enhanced flux pinning by the induced strain. Oberly et al,[136] Hillman et al,[137] Suenaga and Sampson,[139] and Dies et al[140] also observe the initial J_c enhancement in bend tests. Bend strains (total composite) up to 0.5–1.0% can be given to multifilamentary Nb_3Sn composites before any appreciable degradation of J_c is observed.[108,135-141]

Bend tests have also been carried out on V_3Ga,[105,111,139,143] Nb_3Al,[144] V_3Si,[145] $VHf_{0.35}Zr_{0.65}$,[94] and Nb_3Ge.[146] In all cases degradation occurs at bend radii where the compound layer presumably reaches the fracture strain (~ 0.1–0.3%). As already mentioned it has been repeatedly suggested that the C-15 V_2(Hf, Zr) compounds should show more ductility than other compound superconductors because of their lower hardness values. However, bend tests on 100 μm thick $V/Hf_{0.35}Zr_{0.65}$ tape indicate degradation in J_c begins at a diameter of 1.5 cm.[94] This means a strain of $\sim 0.7\%$ at the outer surface of the tape, but since the C-15 compound was in the centre, closer to the neutral axis, a smaller strain would exist in it. Thus, until more detailed tests are carried out, we tentatively conclude that the C-15 V_2(Hf, Zr) compounds do not possess significantly better mechanical

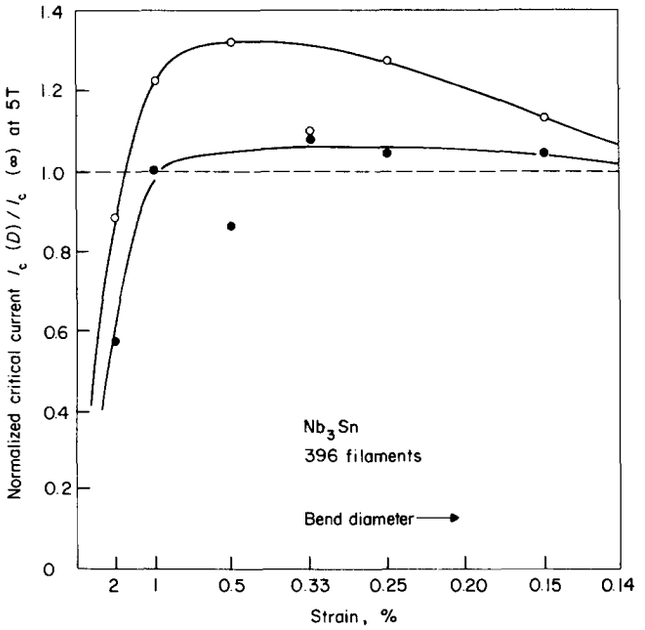

Fig. 26 The degradation of I_c as a result of bending strain in a Nb_3Sn conductor (after Randell et al[135])

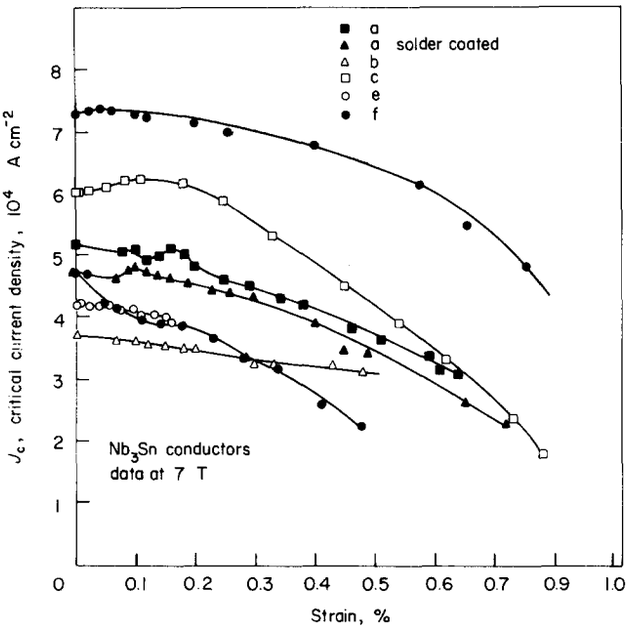

Fig. 27 The effect of strain on J_c for a number of Nb_3Sn multifilamentary conductors

properties than the other high field compound superconductors.

Tensile tests have been conducted on tape composites at both room temperature[102,147] and 4.2 K[102] and subsequent critical currents, J_c, have been measured. Degradation of J_c with tensile strain followed the predictions of Benz[100] and Henning et al,[101] for fracture strain in the compound.

Within the last year, data have become available on the effect of tensile strain on J_c of multifilamentary compound superconductors. McDougall[148] apparently was the first to report such measurements in multifilamentary Nb_3Sn. He measured the degradation in J_c stressed at 4.2 K, and found the critical strain at the onset of degradation to be $\sim$ 50% less at 4.2 K than after straining at room temperature. He found the reaction conditions for Nb_3Sn formation influenced the strain at which degradation in J_c occurred. The conditions that produced a larger Nb_3Sn grain size produced smaller strains for the onset of degradation. Cracking along the grain boundaries was observed. Single filament samples were more resistant to strain degradation than were multifilamentary composites. The critical strain to failure was linearly related to the niobium core diameter when the Nb_3Sn layer thickness and character (grain size, etc) were kept constant. Removing the bronze matrix on the single filament wires decreased the critical degradation stresses by $\sim 1/2$. Filaments from mechanically tested samples were removed by etching away the matrix and studied with scanning electron microscopy (SEM). At strains of $\sim 0.1\%$ the filaments appeared 'polished' suggesting slip in the adjacent matrix. Grain boundary cracks were observed at strains of $\sim 0.4\%$ for 8 μm filaments reacted at 650°C for one hour. This strain corresponded to the observed degradation in J_c. Recovery of J_c occurred after stress removal. The reversible degradation of J_c was attributed to subcritical grain boundary cracks which close on stress removal. Small subcritical cracks might also increase the fluxoid pinning and thus be responsible for the observed initial increase in J_c with stress. In general increasing the filament diameter increased the mechanical support for the Nb_3Sn.

Ekin[149] and Ekin and Clark[121] studied the influence of stress on J_c at magnetic fields to 9.0 T in multifilamentary Nb_3Sn. At high stresses large resistivities were observed by the voltage–current characteristic ($< 10^{-11}\ \Omega$ cm). This presented a problem for the definition of J_c which has subsequently been discussed by Clark and Ekin.[150] A constant axial electric field (3 μV cm^{-1}) was used in this work but other definitions of J_c such as various voltage criteria could lead to a wide variation of J_c values at the same measurement Ekin observed much less degradation in reinforced cables than in unreinforced monolithic conductors, due to the smaller strains in the Nb_3Sn at a given applied stress. The monolithic conductor showed permanent J_c degradation at higher stresses while recovery of 30–70% of the degradation was seen in the cable conductor. Degradation in J_c depends on the applied magnetic field; 5–10% more degradation at 9.0 T than at 7.0 T.

Easton and Schwall[138] compared the degradation in J_c due to tensile stresses at 4.2 K with the results of bend tests at room temperature. An example of the degradation of J_c with tensile strain for a variety of multifilamentary Nb_3Sn conductors is presented in Fig. 27. While strains in the room temperature bend tests of $\sim 0.6\%$ in the outer fibre caused essentially no reduction in J_c, tensile strains of 0.3% produced degradations in J_c of 12–30%. At strains above 0.7%; V–I curves showed large voltages to develop even when I was nearly zero. Unlike similar measurements in Nb-Ti conductors, a large amount of scatter in the J_c degradation was observed, even on samples taken from the same conductor. The initial increase in J_c with stress–strain was observed in some samples but not even in all from the same conductor. Easton[10] also found greater stress-produced degradation in J_c for a sample with no filament twist pitch than in an identical conductor with a twist pitch of 10 mm.

Hillmann et al[137] also carried out tensile and bend tests on multifilamentary Nb_3Sn conductors. They considered the influence of the compressive strains of the bronze matrix on the Nb_3Sn superconducting properties. This in turn depended on the Nb_3Sn layer thickness and composition of the conductors. Hillman et al concluded that the compressive

strains led to degradation of T_c, H_{c_2}, and J_c. At high magnetic fields ($> \sim 8$ T), J_c was lower for samples reacted at lower temperatures, probably due to the lower H_c and T values. Thinner layers of Nb_3Sn produced lower T_c values. Single core Nb_3Sn-Nb composites showed lower T_c values than the multifilamentary material. When the bronze matrix was removed by etching from both types of conductor, T_c increased by as much as 1.5–1.8 K. Tensile tests and bend tests showed an increase in J_c and T_c with initial tensile stress, apparently due to the reduction of the compressive stress. Further tensile stressing led to degradation but recovery in J_c occurred even after 20% degradation. Cracks in the Nb_3Sn layer were not observed at strains below $\sim 1\%$.

Larbalestier et al[109] studied the influence of tensile stress on J_c of multifilamentary Nb_3Sn. The J_c measurements were all made at a field of 3 T. No degradation was observed at stresses up to 10^8 N m^{-2}. At stresses of 2.5×10^8 N m^{-2} a reversible degradation was observed but at higher stresses permanent degradation set in. The value of J_c was too low to be useful for stresses as high as 4.0×10^8 N m^{-2}. Several load cycling experiments were also carried out. Slight increases ($\sim$ 1–2%) in J_c degradation were observed after ten cycles to 2.8×10^8 N m^{-2} with no further changes after four cycles. At higher stresses (for example, 3.35×10^8 N m^{-2}) larger changes in J_c degradation ($\sim$ 13%) were seen after ten cycles. Less degradation in J_c was indicated than that found by some of the other investigations.[138,149] However, since Larbalestier's data were taken at 3 T, the field variation of the degradation observed by Ekin[149] may account for these differences; that is, less stress-induced degradation may be expected at lower magnetic fields. Fisher and Kim[151] investigated the effects of cyclic strain on a composite containing $\sim$ 25, 000 Nb_3Sn filaments in a copper matrix. They found the endurance limit during elastic load-unload cycles to be greater than anticipated. I_c did not degrade for 3850 cycles at strains in the 0.1 to 0.2% range.

The mechanism for the irreversible J_c degradation in multifilamentary Nb_3Sn is probably due to cracking of the filaments when their fracture strain is exceeded. Support for this conclusion comes from several experiments[123,148] using SEM on filaments etched from the matrix after strains into the irreversible J_c degradation regime. However, the mechanism for the reversible J_c degradation has not yet been esolved. Several suggestions for the mechanism have been proposed. McDougall[148] suggested that the reversible degradation, as well as the initial increased in J_c with stress, is caused by subcritical microcracks along the grain boundaries which close when the applied stress is removed. Ekin[123] proposes that the reversible behaviour might be due to either a shift in T_c or H_{c_2} by stress-induced band structure changes and/or martensitic phase transformations, or a stress-induced change in the fluxoid pinning structure. Hillmann et al[137] attribute the decrease in J_c under stress to the corresponding stress-induced degradation of T_c and H_{c_2}. No speculation as the the microstructural mechanism for these changes was given.

Luhman and Suenaga[152] studied the effects of removing the bronze matrix on T_c and J_c in single core bronze-processed Nb_3Sn. The parameters T_c, H_{c_2}, and J_c at high fields (> 10 T) increased on removal of the cladding. This was attributed to a removal of compressive stresses which degrade T_c on the Nb_3Sn. Increases in T_c of $\sim$ 1.2–1.5 K were found and the transition widths decreased from $\sim$ 1.4 to 0.4 K. The decrease in T_c increased with increases in the relative amount of bronze cladding. The change in T_c was $\sim$ ten times greater than predicted from the pressure dependence of T_c in Nb_3Sn. Suggested explanations for this effect were a stress-induced change in order or a stress-induced phase transformation. These results may help explain the reversible tensile stress degradation in Nb_3Sn. However, while J_c increased at high fields (> 10 T) after cladding (stress) removal, the reverse was observed at lower fields (< 10 T). Since the experiments on the tensile stress degradation of J_c have been conducted only at fields < 10 T, a simple correlation of T_c and J_c degradation may not yet be made.

The influence of stress effects on superconducting applications

The design of large superconducting magnets for fusion research and energy storage must consider the limitations imposed by stress effects on superconducting properties. Stress/strain limitations vary from design to design, but typical numbers for maximum stress and strain are: $7 \times 10^7 - 2 \times 10^8$ N m^{-2} and 0.1–0.2% strain.[153,154] At these levels the static degradation of NbTi conductors is negligible. However, if pulsed coil operation results in cyclic stress at long cycle times fatigue failure of the NbTi filaments may become important. Some ($\sim$ 10–15%) degradation can be observed in certain Nb_3Sn composites even at the low design strains ($\sim$ 0.15%) indicated. The degradation in J_c under static stress is then chiefly a problem of providing sufficient mechanical support to the superconductor to minimize the effect of any stress–strain. However, this is not a trivial engineering or economic problem and any lessening of the stress–strain specifications on the superconductor could result in large savings in capital investment.[153]

Stress-induced heat generation in composite superconductors has been studied by Easton et al[155] and Kroeger et al.[156] The source of this heat under pulsed field (therefore stress) conditions is the hysteretic stress–strain loops which develop due to the composite nature of the conductors. Kroeger et al[156] compared the heat generated by stress, obtained from temperature rises, with the work done on the specimen, calculated from the area under the stress–strain curves (Fig. 28). The cases of 'initial loading', that is, where the sample is first plastically deformed, and 'cyclic loading', where the hysteresis loop has been stabilized by repeated stress cycling are both presented. Smaller values of heat were generated as measured calorimetrically than indicated from the stress–strain curves for the 'initial loading' case, because some of the work goes into elastic stored energy. The good agreement between the two measurements for 'cyclic loading' confirms the assumption that after the hysteresis loop is stabilized, all of the mechanical work is converted to heat in the system. Of a number of conductor variables such as number and size of the filaments twist pitch, ratio of normal to superconducting material, etc, only the matrix material appeared to influence the heat generated. An aluminium alloy matrix composite exhibited the substantially lowersheat generation than those with copper matrices. Kuchnir[157] measured stress heating in a thermally insulated NbTi/Cu composite, and found equal temperature rises occurred when the composite was (1) loaded to some stress level, and (2) unloaded to zero stress.

The phenomenon of 'training' has frustrated designers of magnets over the years. 'Training' – the successive increase

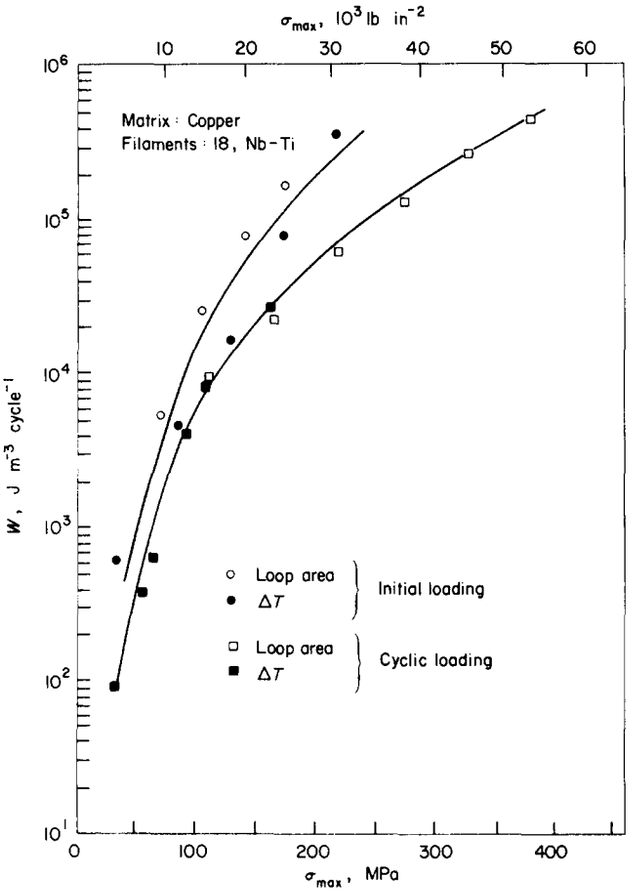

Fig. 28 Comparison of heat generated by stress as obtained from temperature rises to the work done on the specimen found from stress–strain curves for a Nb-Ti/Cu conductor. In initial loading the sample is just plastically deformed; in cyclic loading the hysteresis loop has been stablized by repeated stress cycling

in critical current density with prior testing – has been attributed to a number of causes including a minimization of induced currents,[113] conductor movement, cracking of the impregnant (epoxy), or general movement of the coil.[158]

In spite of a large effort to develop optimum techniques for coil potting, Wilson states (in a recent review on stabilization of superconductors for use in magnets) that ' . . . degraded performance and training are still shown by high current density magnets.[159]

Recently, mechanical effects in the conductor itself have been suggested as the mechanisms responsible for training. Heim[59] proposed that the inelastic deformation of the copper matrix was responsible for training. He recommended a procedure of 'post wind'preload' to erase the mechanical hisotry effects which, due to the Bauschinger effect, had kept the conductor in a condition at or near the matrix yield point. This would involve prestressing the copper to levels above the operational stress. However, Schmidt[11,160] gives arguments against plastic deformation of the copper matrix as the solution for training. His reasons include: (1) training is observed in bare NbTi wires, (2) experimentally, he found the quench to occur before the copper matrix reached the critical temperature, $T_c(J_c, B)$, and (3) that in superconducting magnets training cannot be prevented by slow energizing.

Evans[29] proposed that training is associated with serrated yielding, since significant temperature rises have been recorded during serrated yielding.[27,28] Schmidt[11] dismisses this possible mechanism since he claims the serrations only occur in the plastic portion of the NbTi stress–strain curve at 4.2 K at strains $\gtrsim$ 1%. However, Easton and Koch[17] believe that micro yielding (and thus heating), not shown by a stress–strain curve, can occur at low strains as indicated by acoustic noise. The resolution of the usual stress–strain equipment is not sufficient to detect the microplastic processes which are presumably responsible. Schmidt[160] has studied the stress–strain behaviour at 4.2 K in Nb-Ti with acoustic emission techniques and suggests that microplastic processes (twinning, dislocation motion) are responsible for the training observed in his experiments.

Conclusion

A good start has been made in understanding the mechanical properties of hard superconductors and stress effects on superconducting behaviour. Problem areas have been defined but much research needs to be done. The mechanisms for degradation of J_c in both Nb-Ti and Nb_3Sn must be studied by microstructural techniques. The nature of cyclic stress effects requires further research. The various mechanical effects which may produce heating and instabilities in magnets require study. Consultation between materials scientists, device engineers, and designers will be needed to solve the complex problems in this area. The best solution to the stress effects problem would be the development of a high field superconductor with good strength and especially good ductility even at 4.2 K. Such a superconductor would need to be combined in a composite so that the inelastic effects which generate heat are minimized. But in the absence of such an ideal conductor, careful mechanical/superconducting measurements should be continued on state-of-the-art conductors to set the limitations on the applications of superconducting devices. It is becoming generally recognised[153,161,162] that mechanical effects may be the most severe limitation on the successful use of superconductors in large machines and devices.

This research was sponsored by the Energy Research and Development Administration under contract with Union Carbide Corporation. The experimental work at ORNL was supported by the Superconducting Magnet Development Program of the Magnetic Fusion Energy Division.

The authors wish to extend thanks to C.J. McHargue and R.A. Vandermeer for their reviews and discussion, to the many authors and publishers who have granted permission to call upon their work, and especially to those who have allowed us to include those figures which have been previously published.

References

1 **Reid, C.N., Routbort, J.L., Maynard, R.A.** *J Appl Phys* **44** (1973) 1398
2 **Voigt, W.** Lehrbuch der Kristalphysik (Teubner, Leipzig 1928) 716
3 **Reuss, A.** *Z Angew Math Mech* **9** (1929) 55
4 Rutherford Laboratory, Chilton, England, Central Engineering Group Design Note EDN 0001 (1967)
5 **Reed, R.P., Mikesell, R.P., Clark, A.F.** Advances in Cryogenic Engineering Vol 22 (1977) 463
6 **Nedyukha, M.M., Chernyy, V.G.** *Fiz Metal Metalloved* **22** (1966) 114
7 **Ledbetter** quoted in reference 5
8 **Albert, H., Pfeiffer, I.** *Z für Metallkunde* **63** (1972) 126
9 **Easton, D.S., Koch, C.C.** Advances in Cryogenic Engineering Vol 22 (forthcoming)

10 **Easton, D.S.** unpublished research, Oak Ridge Laboratory (1976)
11 **Schmidt, C.** *Appl Phys Lett* **28** (1976) 463
12 **Fedotov, S.G.** Titanium Science & Technology Vol 22 [R.I. Jaffe and H.M. Burte (eds)] (Plenum Press, New York, 1973) 871
13 **Nelson, C.W., Gibbons, D.F., Hehemann, R.F.** *J Appl Phys* **37** (1966) 4677
14 **Sekula, S.T., Redman, J.K.** unpublished research, Oak Ridge National Laboratory (1961)
15 **Perkins, J.** *Met Trans* **4** (1973) 2709
16 **Baker, C.** *Met Sci J* **5** (1971) 92
17 **Easton, D.S., Koch, C.C.** Shape Memory Effects in Alloys [J. Perkins (ed)] (Plenum Press, New York, 1975) 431
18 **Delaey, L., Krishman, R.V., Tas, H., Warlimont, H.** *J Mat Sci* **9** (1974) 1521
19 **Duwez, P.** *Trans ASM* **45** (1953) 934
20 **Brown, A.R.G., Clark, D., Eastabrook, J., Jepson, K.S.** *Nature* **201** (1964)
21 **Read, D.** private communication, NBS Boulder (1977)
22 **Easton, D.S., Koch, C.C. , Kroeger, D.M.** research in progress, Oak Ridge National Laboratory (1977)
23 **Wigley, D.A.** Mechanical Properties of Materials at Low Temperatures (Plenum Press, New York, 1971) 23
24 **Blewitt, T.H., Coltman, R.R., Redman, J.K.** *J Appl Phys* **28** (1957) 651
25 **Collins, S.C., Ezekial, F.O., Sepp, O.W., Rizika, J.W.** *Proc ASTM* **56** (1956) 687
26 **Wessel, E.T.** *Trans ASM* **49** (1957) 149
27 **Basinski, Z.S.** *Proc Roy Soc* **A240** (1957) 229
28 **Basinski, Z.S.** *Aust J Phys* **13** (1960) 354
29 **Evans, D.** Rutherford Laboratory Report RL-73-092 (1973)
30 **Hillmann, H.** Federal Republic (of W. Germany) Ministry of Research and Technology, Research Report T 73-03 (1973)
31 **Albert, H., Pfeiffer, I.** *Metallkde* **67** (1976) 356
32 **Yajima, M., Ishill, M.** *J Japanese Met Soc* **31** (1967) 664
33 **Flewitt, P.E.J., Palmer, D.E.B.** *J Less Common Met* **32** (1973)
34 **Verkin, B.I., Parkhomenko, T.A., Pustovalov, V.V., Startsev, V.I.** 'Low temperature plasticity of niobium–titanium superconducting materials' Academy of Sciences of the Ukranian SSR Physico-Technical Institute of Low Temperatures (1975)
35 **Reed, R.P., Mikesell, R.P.** *J Mater* **2** (1967)
36 **Reed, R.P., Mikesell, R.P.** 'Tensile properties of superconductors' paper presented at Symposium on Stress Effects in Superconductors (Vail, Colorado, 1976)
37 **Wigley, D.A.** Mechanical Properties of Materials at Low Temperatures (Plenum Press, New Yor, 1971) 88
38 **Fox, D.K., Pryle, W.H.** Advances in Cryogenic Engineering Vol 9 (Plenum Press, New York, 1964) 124
39 **Bychkova, M.I., Baron, V.V., Savitskii, E.M.** Physics and Metallurgy of Superconductors [Savitskii, E.M., Baron, V.V. (eds)] (English Translation by D.G. Archard) (Consultants Bureau, New York, 1970) 53
40 **Bychkova, M.I., Baron, V.V., Savitskii, E.M.** Physics and Metallurgy of Superconductors (Consultants Bureau, New York, 1970) 90
41 **Alekseevskii, N.E., Pubrovin, A.V., Mikhailov, N.N., Sokolov, V.I., Fedotov, L.N.** *Soviet Phsyics – Daklady* **11** (1957) 993
42 **Takaai, T.** *J Japan Met Soc* **32** (1968) 802
43 **Courtney, T.H., Wulff, J.** *Phys Lett* **25A** (1967) 477
44 **Neal, D.F., Barber, A.C., Woolcock, A., Gidley, J.A.F.** *Acta Metall* **19** (1971) 143
45 **Pfeiffer, I., Hillmann, H.** *Acta Metall* **16** (1968) 1429
46 **Reuter, F.W., Ralls, K.M., Wulff, J.** *Trans Metall Soc AIME* **236** (1966) 1143
47 **Witcomb, M.J., Dew-Hughes, D.** *J Mat Sci* **8** (1973) 1383
48 **Baker, C.,** *J Mat Sci* **5** (1970) 40
49 **Walker, M.S., Stickler, R., Werner, F.E.** 'Metallurgy of advanced electronic materials' Met Soc AIME [G.E. Brock (ed)] (Interscience, New York, 1963) 49
50 **Milne, I.** *J Mat Sci* **7** (1972) 413
51 **Narlikar, A.V., Dew-Hughes, D.** *J Mat Sci* **1** (1966) 317
52 **Finlayson, T.R., Milne, I.** *J Mat Sci* **7** (1972) 1391
53 **Livingston, J.D.** Proc Summer Study on Superconducting Devices and Accelerators, Part 2, BNL (1968) 377
54 **Kelly, A., Davies, G.J.** *Metall Rev* **10** (1965) 1
55 **Kelly, A.** Strengthening Methods in Crystals [A. Kelly and Nicholson, R.B. (eds)] (Applied Science Publishers Ltd, London, 1971) 433
56 **Lawley, A., Koczak, M.J.** Tech Report #7, Office of Naval Research, Constract #N00014-67-A-0406-001 (March 1972)
57 **Stowell, E.Z., Liu, T.S.** *J Mech Phys Sol* **9** (1961) 242
58 **Kelly, A.** Strong Solids, 2nd edn (Clarendon Press, Oxford, 1973) 215
59 **Heim, J.R.** Report No TM-334-B, Fermi National Accelerator Laboratory (1974)
60 **Piehler, H.R.** *Trans Met Soc AIME* **233** (1965) 12
61 **Fisher, E.S., Kim, S.H., Turner, A.P.L.** Proc ICEC6 (IPC Science & Technology Press, 1976) 390
62 **Fedor, R.J., Ebert, L.J.** *J Eng Mat Tech: Trans ASME* (April, 1973) 69
63 **Weger, M., Goldberg, I.B.,** Solid State Phys [Seitz, F., Turnball, D. (eds)] (Academic Press, New York, 1973) 28
64 **Testardi, L.R.** Physical Acoustics [Mason, W.P., Thurston, R.N. (eds)] (Academic Press, New York, 1973) 93
65 **Testardi, L.R.** *Rev Mod Phys* **47** (1975) 637
66 **Testardi, L.R., Reed, W.A., Bateman, R.B., Chirba, V.G.** *Phys Rev Lett* **15** (1965) 250
67 **Rehwold, W., Royl, M., Cohen, R.W., Cody, G.D.** *Phys Rev B* **6** (1972) 363
68 **Batterman, B.W., Barrett, C.S.** *Phys Rev* **145** (1966) 296
69 **Mailfert, R., Batterman, B.W., Hanak, J.J.,** Phys Lett A **24** (1967) 315; *Phys Status Solidi* **32** (1969) K67
70 **Nembach, E., Tachikawa, K., Takano, S.** *Phil Mag* **8** (1970) 869
71 **Kodess, B.N. , Kurithzin, V.B., Tretjakov, B.N.** *Phys Lett A* **37** (1971) 415
72 **Noolandi, J., Varma, C.M.** *Phys Rev B* **11** (1975) 4743
73 **Patel, J.R., Batterman, B.W.** *J Appl Phys* **37** (1966) 3447
74 **Patel, J.R., Batterman, B.W.** *Phys Rev* **148** (1966) 662
75 **Vance, E.R., Finlayson, T.R.** *J Appl Phys* **39** (1968) 1980
76 **Finlayson, T.R., Vance, E.R., Rachinger, W.A.** *Phys Lett A* **26** (1968) 474
77 **King, H.W., Cocks, F.H., Pollock, J.T.A.,** *Phys Lett A* **26** (1967) 77
78 **Old, C.F., Charlesworth, J.P.** *Cryogenics* **16** (1976) 469
79 **Carcia, P.F., Barsch, G.R.,** *Phys Stat Sol B* **59** (1973) 595
80 **Chu, C.W., Testardi, L.R.** *Phys Rev Lett* **32** (1974) 766
81 **Blaugher, R.D., Taylor, A., Ashkin, M.** *Phys Rev Lett* **33** (1974) 292
82 **Testardi, L.R., Chu, C.W.** *Phys Rev B* **15** (1977) 146
83 **Smith, T.F., Finlayson, T.R., Shelton, R.N.** *J Less Common Met* **43** (1975) 21
84 **Smith, T.F., Finlayson, T.R., Taft, A.** *Comm on Phys* **1** (1976) 167
85 **Lawson, A.C., Zachariasen, W.H.** *Phys Lett* **38A** (1972) 1
86 **Moncton, D.E.** *Solid Stat Comm* **13** (1973) 1779
87 **Finlayson, T.R., Thomson, K.W., Smith, T.F.,** *J Phys F Met Phys* **5** (1975) L225
88 **Doherty, J.E., Gibbons, D.F.** *Phys Stat Solidi* **44** (1971) K5
89 **June, C.K. Shaffer, P.T.B.** *J Less Common Met* **23** (1971) 367
90 **Smith, W.D., Lin, R.Y., Coppola, J.A., Economy, J.** *IEEE Trans on Magnetics* **MAG-11 (1975)** 182
91 **Pike, G.E., Mullendore, A.W., Schirber, J.E., Napier, J.** *IEEE Trans on Magnetics* **MAG-11** (1975) 162
92 **Levinstein, H.J., Greiner, E.S., Mason, H., Jr** *J Appl Phys* **37** (1966) 164
93 **Inoue, K., Tachikawa, K., Iwasa, Y.,** *Appl Phys Lett* **18** (1971) 235
94 **Inoue, K., Kawanura, H., Tachikawa, K.,** Proc ICEC5 Kyoto, (1974) p 336
95 **Kunzler, J.E., Buehler, E., Hsu, F.S.L., Wernick, J.H.** *Phys Rev Lett* **6** (1961) 89
96 **Buehler, E., Wernick, J.H., Olsen, J.M., Hsu, F.S.L., Kunzler, J.E.** Metallurgy of Advanced Electronic Materials [Brock, G.E. (ed)] (Interscience Publishers, 1963) 105
97 **Hanak, J.J.** Metallurgy of Advanced Electronic Materials (1963) 161
98 **DeSorbo, W.** *Cryogenics* **4** (1964) 218
99 **Benz, M.G.** *IEEE Trans Magn* **MAG-2** (1966) 760
100 **Benz, M.G.** *J Appl Phys* **39** (1968) 2533
101 **Henning, C.D., Nelson, R.L., Leichter, H.L., Ward, C.O.** Int Conf Magnet Tech BNL (1972) 521
102 Power Transmission Project Quarterly Report, PTP No 29; Brookhaven National Laboratory (1974)
103 **Suenaga, M., Sampson, W.B., Klamut, C.J.** *IEEE Trans Magn* **MAG-11** (1975) 231
104 **Suenaga, M., Sampson, W.B.** *Appl Phys Lett* **18** (1971) 584
105 **Furoto, Y., Suzuki, T., Tachikawa, K., Iwaso, Y.** *Appl Phys Lett* **24** (1974) 34

106 **Howe, D.G., Weinman, L.S.** *Appl Polymer Symp* **29** (John Wiley, 1976) 25
107 **Vandervoort, R.R.** Lawrence Livermore Laboratory, Internal Memorandum (1975)
108 **McDougall, I.L.** *IEEE Trans Magn* **MAG-11** (1975) 1467
109 **Larbalestier, D.C., Magraw, J.E., Wilson, M.N.** *IEEE Trans Magn* **Mag-13** (1977) 462
110 **Tsuei, C.C., Suenaga, M., Sampson, W.B.** *Appl Phys Lett* **25** (1974) 318
111 **Tanaka, Y., Furuto, Y.** The Furukawa Electric Co Ltd, Tokyo (forthcoming publication)
112 **Easton, D.S., Taylor, P.A.** research in progress, Oak Ridge National Laboratory (1976)
113 **Livingston, J.D., Schadler, H.W.** *Progr Mat Sci* **12** (1964) 249
114 **Garland, J.W., Bennemann, K.H.** Superconductivity in d- and f-Bond Metals [**Douglass, D.H.** (ed)] AIP Conf Proc 4 (AIP, New York, 1972)
115 **Ho, J.C., Collings, E.W.** *J Appl Phys* **42** (1971) 5144
116 **Finlayson, T.R., Milne, I.** *Solid State Comm* **9** (1971) 1339
117 **Campbell, A.M., Evetts, J.E.** *Adv Phys* **21** (1972) 199
118 **Kostorz, G.** *Phys Status Solidi B* **58** (1973) 9
119 **Ekin, J.W., Fickett, F.R., Clark, A.F.** *Advances in Cryogenic Engineering* **22** (1977) 449
120 **Easton, D.S., Koch, C.C.** Magnetic-Fusion Energy Materials Technology Programme Annual Progress Report for Period Ending June 30 1976, ORNL-5189 (1976) 63
121 **Ekin, J.W., Clark, A.F.** AIP Conf Proc Joint MMM Intermag Conf, Pittsburgh, Pa (1976)
122 **Klamut, C., Suenaga, M.** Unpublished research, Brookhaven National Laboratory (1976)
123 **Ekin, J.W.** *IEEE Trans on Magn* **Mag-13** (1977) 127
124 **Müller, C.B., Saur, E.** Advances in Cryogenic Engineering Vol 8 (1963) 574
125 **Pupp, W.A., Sattler, W.W., Saur, E.J.** *J Low Temp Phys* **14** (1974) 1
126 **McEnvoy, J.P.** Proc of Int Conf on the Science of Superconductivity (1969) [**Chilton, F.** (ed)] (North-Holland, Amsterdam, 1971) 540
127 **Weger, M., Silbernagel, B.G., Greiner, E.S.** *Phys Rev Lett* **13** (1964) 521
128 **Müller, C.B., Saur, E.J.** Advances in Cryogenic Engineering Vol 9 (1963) 338
129 **Buehler, E., Levinstein, H.J.** *J Appl Phys* **36** (1965) 3856
130 **Pulver, M.** *Z Physik* **257** (1972) 261
131 **Brand, R., Webb, W.W.** *Solid State Comm* **7** (1969) 19
132 **Matthias, B.T., Corenzwit, E., Cooper, A.S., Longinotti, L.D.** *Proc Nat Acad Sci* **68** (1971) 56
133 **McCarthy, S.L.** *J Low Temp Phys* **4** (1971) 669
134 **Smith, T.F.** *J Low Temp Phys* **6** (1972) 171
135 **Randell, R., Wong, J., Deis, D.W., Shaw, B.J., Daniel, M.R.** *IEEE Trans Magn* **MAG-11** (1975) 291
136 **Oberly, C.E., Ohmer, M.C., Gegel, H.L.** Proc 5th Int Conf on Magnet Technology (MT-5) Rome, 1975, CNEN [**Sacchetti, N., Spadoni, M., Stipcich, S** (eds)] (1975) 704
137 **Hillmann, H., Kuckuck, H., Pfister, H., Rupp, G., Springer, E., Wilhelm, M., Wohllehen, K., Ziegler, F.** *IEEE Trans on Magn* **Mag-13** (1977) 792
138 **Easton, D.S., Schwall, R.E.** *Appl Phys Lett* **29** (1976) 319
139 **Suenaga, M., Sampson, W.B.** *Appl Phys Lett* **20** (1972) 443
140 **Deis, D.W., Gavaler, J.R., Shaw, B.J.** *J Appl Phys* **45** (1974) 4594
141 **Scanlan, R.M., Fietz, W.A.** *IEEE Trans on Magn* **MAG-11** (1975) 287
142 **Tanaka, Y., Furuto, Y., Ikeda, M., Inoue, I., Tanii, J.,** Proc ICEC6 (IPC Science & Technology Press, 1976) 381
143 **Ikeda, M., Furuto, Y., Tanaka, Y., Inoue, I., Ban, M.** Proc ICEC5 (IPC Science & Technology Press Ltd, 1974) 329
144 **Ceresara, S., Ricci, M.V., Sacchetti, N., Sacerdoti, G.** *IEEE Trans on Magn* **MAG-11** (1975) 263
145 **Suenaga, M., Sampson, W.B.** Proc of 1972 Applied Superconductivity Conference (1972) 481
146 **Braginski, A.I., Manser, S.F., Roland, G.W., Burghardt, R.R., Daniel, M.R., Janocko, M.A.** An improved Superconductor for Transmission Line Applications, Phase I, Final Report Westinghouse Electric Corp., Pittsburgh, Pennsylvania, ERDA, contract No E(11-1)-2522 (1975)
147 **Dickinson, J.M., Jones, T.I., Bartlett, R.J.,** unpublished research, Los Alamos Scientific Laboratory (1976)
148 **McDougall, I.L.** Proc ICEC6 (IPC Science & Technology Press, 1976) 396
149 **Ekin, J.W.** *Appl Phys Lett* **29** (1976) 216
150 **Clark, A.F.** *IEEE Trans on Magn* **Mag-13** (1977) 38
151 **Fisher, E.S., Kim, S.H.** *IEEE Trans on Magn* **Mag-13** (1977) 112
152 **Luhman, T., Suenaga, M.** *Appl Phys Let* **29** (1976) 61
153 **Young, W.C., Boom, W.R.** Proc 4th Conf on Magnet Technology, Brookhaven (1972) 244
154 Workshop on Large Coil Project, Thermonuclear Division, ORNL, (1976)
155 **Easton, D.S., Kroeger, D.M.** *Appl Phys Lett* **29** (1976) 382
156 **Kroeger, D.M., Easton, D.S., Moazed, A.** *IEEE Trans on Magn* **Mag-13** (1977) 120
157 **Kuchnir, M.,** unpublished research, Accelerator Laboratory, presented at Symposium on Stress Effects in Superconductors, Vail, Colorado (1976)
158 **Wilson, M.N.** *Composites* (1970) 341
159 **Wilson, M.N.** *IEEE Trans on Magn* **Mag-13** (1977) 440
160 **Schmidt, C., Pasztor, G.** *IEEE Trans on Magn* **Mag-13** (1977) 116
161 **Komarek, P.** *Cryogenics* **16** (1976) 131
162 **Wilson, M.N.** Proc 5th Int Conf on Magnet Tech (MT-5), Rome, Italy, (April, 1975) [**Sacchetti, N., Spadomi, M., Stipcich, S.** (eds)] (Laboratory Nazionali del CNEN, 1975) 615